

NASA/TM—2001-210674



Effect of Delta Tabs on Free Jets from Complex Nozzles

K.B.M.Q. Zaman
Glenn Research Center, Cleveland, Ohio

March 2001

The NASA STI Program Office . . . in Profile

Since its founding, NASA has been dedicated to the advancement of aeronautics and space science. The NASA Scientific and Technical Information (STI) Program Office plays a key part in helping NASA maintain this important role.

The NASA STI Program Office is operated by Langley Research Center, the Lead Center for NASA's scientific and technical information. The NASA STI Program Office provides access to the NASA STI Database, the largest collection of aeronautical and space science STI in the world. The Program Office is also NASA's institutional mechanism for disseminating the results of its research and development activities. These results are published by NASA in the NASA STI Report Series, which includes the following report types:

- **TECHNICAL PUBLICATION.** Reports of completed research or a major significant phase of research that present the results of NASA programs and include extensive data or theoretical analysis. Includes compilations of significant scientific and technical data and information deemed to be of continuing reference value. NASA's counterpart of peer-reviewed formal professional papers but has less stringent limitations on manuscript length and extent of graphic presentations.
- **TECHNICAL MEMORANDUM.** Scientific and technical findings that are preliminary or of specialized interest, e.g., quick release reports, working papers, and bibliographies that contain minimal annotation. Does not contain extensive analysis.
- **CONTRACTOR REPORT.** Scientific and technical findings by NASA-sponsored contractors and grantees.

- **CONFERENCE PUBLICATION.** Collected papers from scientific and technical conferences, symposia, seminars, or other meetings sponsored or cosponsored by NASA.
- **SPECIAL PUBLICATION.** Scientific, technical, or historical information from NASA programs, projects, and missions, often concerned with subjects having substantial public interest.
- **TECHNICAL TRANSLATION.** English-language translations of foreign scientific and technical material pertinent to NASA's mission.

Specialized services that complement the STI Program Office's diverse offerings include creating custom thesauri, building customized data bases, organizing and publishing research results . . . even providing videos.

For more information about the NASA STI Program Office, see the following:

- Access the NASA STI Program Home Page at <http://www.sti.nasa.gov>
- E-mail your question via the Internet to help@sti.nasa.gov
- Fax your question to the NASA Access Help Desk at 301-621-0134
- Telephone the NASA Access Help Desk at 301-621-0390
- Write to:
NASA Access Help Desk
NASA Center for Aerospace Information
7121 Standard Drive
Hanover, MD 21076

NASA/TM—2001-210674



Effect of Delta Tabs on Free Jets from Complex Nozzles

K.B.M.Q. Zaman
Glenn Research Center, Cleveland, Ohio

National Aeronautics and
Space Administration

Glenn Research Center

March 2001

Acknowledgments

The experiments with the ACE nozzle model were planned and conducted in consultation with Dr. J.M. Seiner of NASA LaRC who is closely familiar with the full scale.

Note that at the time of research, the NASA Lewis Research Center was undergoing a name change to the NASA John H. Glenn Research Center at Lewis Field. Both names may appear in this report.

Available from

NASA Center for Aerospace Information
7121 Standard Drive
Hanover, MD 21076
Price Code: A04

National Technical Information Service
5285 Port Royal Road
Springfield, VA 22100
Price Code: A04

Available electronically at <http://gltrs.grc.nasa.gov/GLTRS>

EFFECT OF DELTA TABS ON FREE JETS FROM COMPLEX NOZZLES

K.B.M.Q. Zaman
National Aeronautics and Space Administration
Glenn Research Center
Cleveland, Ohio 44135

Introduction:

The effect of tabs, or small protrusions in the flow placed at the exit of a nozzle, on the evolution and spreading of free jets has been under investigation at NASA Lewis Research Center. The tabs introduce streamwise vortices in the flow which can increase the jet spreading significantly. The streamwise vorticity generation mechanism, and the resultant effect on spreading, noise, thrust loss, etc., for axisymmetric jets have been studied in detail and the results summarized in Ref. 1 (see also, Refs. 2-4).

With non-axisymmetric, e.g., rectangular or elliptic, nozzles the effect of the tabs becomes relatively more complex.^{5,6} It is found that, depending on the nozzle geometry and placement of the tabs, jet spreading can either be increased or decreased. In such jets streamwise vortices are usually already present due to secondary flow within the nozzle. The vortices produced by the tabs then interact with the already present vortices and, depending on the sense and the strength of the resultant vortices, the subsequent evolution of the jet may be affected differently. The phenomenon of axis switching in such jets can also be stopped or promoted depending on the placement of the tabs.⁶ These observations underscore the powerful role of the streamwise vortices in the evolution of free jets.

On the other hand, it should be borne in mind that practically all the vorticity shed initially from the nozzle is azimuthal. Even with the tabs, the intensity of the azimuthal vorticity at any downstream location usually far exceeds the intensity of the streamwise component; the peak of ω_θ is typically measured to be about 5 times larger than the peak of ω_x .⁵ Thus, any process which organizes the azimuthal vorticity and leads to the formation of coherent vortical structures can also have a profound effect on the jet evolution. The influence of the dynamics of the streamwise and azimuthal vortices and their interaction on jet spreading is currently being further investigated.⁷

While carrying out the aforementioned studies of a fundamental nature, efforts have also been made simultaneously to apply the tabs to more complex nozzles of practical interest. In

support of the High Speed Research (HSR) program, experiments have been carried out using simplified models of nozzles that are candidates for the High Speed Civil Transport (HSCT) aircraft. The purpose of the present report is to summarize and document the results obtained with the latter nozzles.

A primary goal in the HSCT program is jet noise reduction with acceptable performance loss. All nozzle configurations considered in the program utilize ejectors. A basic concept in such a configuration is to mix the primary jet with the lower speed outer stream so that a lower velocity at the end of the ejector is obtained. For a given thrust, the lower exhaust velocity results in lower jet noise. The penalty, of course, is larger and heavier nozzle hardware. Therefore, a goal in the design of such a nozzle is to mix the primary jet as fast as possible so that the length and the weight of the ejector can be reduced. Improved mixing within the ejector could also result in additional noise benefit through removal of 'hot spots', i.e., isolated pockets of high velocity fluid. It was thought that the tabs might be helpful in achieving such goals, and this led to the present experiments.

In terms of jet noise reduction, the tabs could have further beneficial effects. They could reduce screech associated noise --an effect that has been well known.⁸ Also, the tabs could be applied at the end of the ejector to increase the spreading of the resultant jet exhaust. It is possible, even though not completely clear, that this might produce some direct noise benefit. That an increased spreading of a free jet produces less noise has been indicated by the analytical study of Ref. 9. The experimental results on the effect of tabs on far field noise of axisymmetric jets, reported in Ref. 10, also lend support to this notion.

The aim in the present experiments has been to look for and demonstrate increased mixing with models of the HSCT primary nozzles through the use of tabs. The bulk of the experiments have been of a trial and error nature, in view of the flow complexities even with the simplified models of the nozzles. The results do show some promise. Only the more promising tab configurations are investigated in detail in regards to jet spreading, noise and thrust loss, and are reported in the following. Obviously, the effectiveness of the tabs cannot be confidently predicted, and tests must be conducted with full scale hardware which will be even more complex involving hot flow and the ejector. The main objective in the present effort has been to come up with recommendations for tab configurations for possible full scale verification.

Models of two nozzles have been considered. One is the lobed mixer nozzle used in most of the configurations considered for the HSCT. The other is an axisymmetric plug case simulating the 'ACE' (Axisymmetric Coannular Ejector) nozzle which is also a candidate for the HSCT. Because of the basic differences in the two nozzle shapes, the results are presented in two parts. Part A documents data obtained with several models of the lobed nozzle. Part B documents those obtained with the 'ACE' nozzle model with various designs of the plug.

Nomenclature:

Cf_1 = Measured thrust normalized by ideal thrust obtained from measured mass flux and NPR, by assuming convergent, uniform flow.

Cf_2 = Measured thrust normalized by ideal thrust obtained from measured mass flux and NPR, by assuming ideal expansion.

D = Equivalent diameter based on nozzle exit area.

d = Diameter of end hole on a porous plug.

\dot{m} = Mass flux at a given x .

\dot{m}_e = Mass flux at nozzle exit estimated for a given NPR assuming uniform flow.

M_j = Jet Mach number had the flow expanded fully for a given NPR.

NPR = Nozzle pressure ratio (P_t/p_a).

P_t = Plenum chamber pressure.

p_a = Ambient pressure.

T = Jet thrust; 'ideal' is isentropic prediction assuming convergent, uniform flow.

U, V, W = streamwise, transverse and spanwise mean velocities.

u', v', w' = turbulent normal stresses.

$\bar{u}v, \bar{u}w$ = Turbulent shear stresses.

U_j = Jet velocity at nozzle exit.

x, y, z = streamwise, transverse and spanwise coordinates.

ω_x = Mean streamwise vorticity, $\partial V/\partial z - \partial W/\partial y$.

Lobed nozzle notations: six-lobed #1 has an end wall at the exit, six-lobed #2 has thin lip and outside chutes cut out.

Plug notations: 'xx%H' or 'xx%S' means plug with xx% surface porosity with 'H' for circular holes providing the porosity and 'S' for slots providing the porosity. A total of five plugs with 10° half-angle are used: one is solid, one is with slots and 10% porosity, others are with holes with porosities of 3.6%, 5.5% and 8.2%. 'Ace_8.2%H_05' denotes nozzle with 8.2% porous plug and $d = 0.05$ inch end hole.

Tab notations: 'nn_a%' denotes equally spaced nn delta tabs with a total area blockage of a%. Three tab configurations are used with 6, 12 and 24 tabs, each with a total area blockage of 4%. Two other configurations are used with 6 and 24 tabs, each with a total area blockage of 1%. '12_4%' tab denotes 12 delta tabs with 4% total area blockage.

Experimental Facilities:

The experiments were conducted in the jet facilities housed in ERB CW13 and CW17. All nozzles studied were convergent ones, converging from a round inlet to the specific exit geometries; a length of approximately 1.27 cm with constant cross section was allowed before the exit. All jets discharged into the ambient of the test cell. Laboratory air supply was used and the flows were continuous with feedback control for holding a set Mach number. Flow field measurements were taken by automated probe traversing mechanisms under computer control.

The smaller jet facility in CW13 was used for much of the earlier work on the tab effect which have been reported in Refs. 1 and 2. In short, this facility has a 11 cm diameter plenum chamber supplied with compressed air with maximum available tank pressure of 80 psig (560 kPa). Nozzles used with this facility have equivalent diameters, $D = 1.47$ cm. Mass flow rate could be measured with an orifice meter fitted to the supply line. Jet thrust could also be measured using a load cell and an auxiliary plenum mounted on linear bearings. All flow visualizations and jet noise measurements were done in this facility.

The larger jet facility is housed in cell CW17. It has a 76 cm diameter plenum chamber fitted with flow conditioning units and an acoustic treatment section. A maximum plenum pressure of 125 psig (875 kPa) and flow rates more than 3.6 kg/sec are available. All nozzles used in this facility for the present experiments have equivalent diameter, $D = 6.35$ cm. The hot-wire measurements for the flow fields were done at a nominal Mach number, $M_j = 0.31$. Limited data were also obtained in this facility at supersonic conditions.

The hot-wire measurements involved use of two crossed wire probes, one in the u-v and the other in the u-w configurations. The probe traversing was done such that the two probes went through the same grid points on a cross sectional plane at a given downstream location. The measurements provided distributions of U , V , W , u' , v' , w' , \overline{uv} and \overline{uw} . Gradients of V and W yielded streamwise vorticity, ω_x . Standard Pitot probe measurements were carried out. The Pitot probe data for the supersonic jets, obtained far enough downstream where the flow was subsonic, provided the Mach number distributions on cross sectional planes. Integration of these data provided streamwise mass fluxes. Further details of the measurement techniques can be found in Refs. 1 and 3.

PART A LOBED MIXER NOZZLE

Fig. A1: The exit section of the large jet facility is shown in (a); the coordinate system used in this report is also indicated. The shape of a 'delta tab', fitted to a circular nozzle, is shown in (b). This is a shape which was reached after some parametric study to produce maximum flow field distortion for a given area blockage. Unless otherwise stated, a 'tab' will imply a 'delta

tab' with dimensions $w/D \approx 0.28$ and $\phi \approx 135^\circ$. The corresponding area blockage per tab is approximately 1.7% of the nozzle exit area.

Two geometries for the lobed nozzle were tested. The smaller, six lobed nozzle had $D = 1.47$ cm and its exit geometry is shown in (c). Two versions of this nozzle were used. One (#1) had a cylindrical outer shape with a diameter of about 5.7 cm; the face of the cylinder at the exit plane formed an 'end wall'. A retainer disc was attached to the end wall to hold the tabs. The second one (#2) had exactly the same interior dimensions as #1, however, the outside was shaved so that the nozzle ended with a thin lip. Thus, this nozzle had the outside chutes cut out through which there was some secondary flow via natural entrainment. The six lobed nozzles were fabricated by EDM.

The other, larger, eight lobed nozzle had similar exit dimensions as a Pratt & Whitney nozzle (NASA Contract No. NAS3-25952; see also Ref. 11). The model had $D = 6.35$ cm, and only the exit dimensions were to scale to approximately simulate the primary flow of the P&W nozzle but the interior shape was arbitrary. The interior converged from 13.3 cm dia round shape to the exit shape; the exit dimensions are shown in (d). This nozzle also had an end wall for easy installation and location of the tabs. In the following, this nozzle is referred to as the P&W nozzle. It was fabricated by stereolithography.

Fig. A2: Two views of the P&W nozzle are shown. In the lower picture the retainer can be seen holding one tab on each side.

Fig. A3: Mach number contours for a supersonic flow at $x/D = 14$, measured with a Pitot probe in the large jet facility, are shown in this figure. Data for the P&W nozzle are compared with those from a circular nozzle fitted with four delta tabs. The circular nozzle had the same exit area ($D = 6.35$ cm).

The contrast is dramatic. An underlying concept for a lobed nozzle is to stretch the mixing layer region exposed to the ambient so that there is more entrainment and spreading. However, it is clear that in regards to that objective the action of the tabs with the circular jet outperforms the lobed nozzle under consideration. In fact, the normalized mass flux for the lobed nozzle was found to be smaller than that for the circular nozzle even without the tabs. The normalized flux values are indicated by the numbers in parentheses on the lower center of these figures. The flux data are further discussed with the next figure. It is noteworthy here that four delta tabs (of the given size and dimension) with the circular nozzle were found to be the optimum for increasing jet spreading.¹ Equally spaced delta tabs with numbers either more or less than four resulted in less spreading.

Fig. A4: The variation of the normalized mass flux with streamwise distance was measured in the small jet facility. Data for the circular jet with and without four delta tabs are compared with those for the six lobed nozzle case. The two solid data points correspond to the large jet case shown in fig. A3 ('cross' for the P&W nozzle, 'plus' for the circular jet with four delta tabs). Even though the normalized fluxes were somewhat lower for the larger nozzles, it is clear that the data trends are essentially independent of Reynolds number which varied by almost a factor of 5 between the two facilities ($Re_D = 4.2 \times 10^6$ for the large jet). Also, as mentioned in the foregoing, the fluxes for the lobed nozzles are found to be consistently lower than even the baseline circular jet case.

The result that the lobed nozzles produce less jet spreading compared to the circular nozzle came as a total surprise. Eventually the reason became apparent. At the given Mach number the circular jet went through a screech, whereas there was no screech with the lobed nozzles. (Noise spectra for the six lobed nozzle will be shown in comparison with the ACE nozzle data in Part B). A screeching jet is a periodically forced jet in which mixing enhancement can take place by an organization of the azimuthal vortical structures. Such an effect has been demonstrated by acoustic forcing of subsonic jets in several previous studies (e.g. Ref. 12). Thus, the presence of screech with the circular nozzle and the absence thereof with the lobed nozzles is believed to have caused the anomaly noted in the foregoing.

As expected, data for the same nozzles of fig. A4, at a subsonic condition (not shown here for brevity), do show a reversal of the trend with the fluxes for the lobed nozzle exceeding that for the circular case. The fluxes for the circular jet with four delta tabs, however, remain by far the largest even at the subsonic condition. Note that the nozzle configuration with the delta tabs in figs. A3 and A4 does not involve any screech and the mixing increase occurs through a different mechanism, i.e., through the dynamics of the streamwise vortices. It may be of interest to note here that at $M_j = 1.63$ the circular jet goes through a screech in the helical mode (mode C).¹³ Screech in the flapping modes (B and D), at higher or lower values of M_j , results in a further increase in jet spreading. These results will be further analyzed and discussed in a later publication.

It should be noted here that the circular jet with four delta tabs is one of the few configurations, found so far, which result in such a large increase in jet spreading. The fluxes obtained are larger than those obtained with the lobed nozzles or non-axisymmetric (e.g., elliptic) nozzles. This is true for supersonic as well as subsonic conditions. Also, at subsonic conditions the increase in the fluxes caused by four tabs far exceeds that achieved by acoustic excitation. Comparison with data for elliptic jets (Refs. 14,15) and acoustic excitation (Ref. 12) has been discussed in Ref. 1.

Fig. A5: The lower flux values measured with the lobed nozzle at first led to the notion that the blockage due to boundary layer thickness in the narrow channels could be high. If that were the case the initial mass flux would be lower, causing the anomaly, as \dot{m}_c , the normalizing quantity, was calculated assuming uniform flow (zero boundary layer thickness). However, if this were the case jet thrust would also be correspondingly lower. The thrust data shown in fig. A5 disproved this notion. Both versions of the six lobed nozzle produced thrusts only slightly lower than that expected from the 'ideal' which was also calculated assuming uniform flow.

The thrust data obtained by using six tabs with the lobed nozzle is also shown in this figure. The tab locations are indicated and the sizes are given in the following with the discussion of fig. A7. At NPR = 4.47 ($M_j = 1.63$), the thrust loss from 'ideal' is found to be about 1.6% for the no tab cases and 6.5% for the six tab case. It should be noted that these thrust loss numbers are overestimates of the performance loss. With the tabs there is flow blockage and for the same NPR the actual mass flow through the nozzle is lower. The appropriate quantifier in this connection is the coefficient of performance (cf1 or cf2). These measurements were done for the ACE nozzle and will be discussed in Part B. The coefficients cf1 and cf2 were not measured in the experiments with the six lobed nozzles. However, a rough estimate for the percent performance loss could be obtained by subtracting the percent area blockage from the percent thrust loss. Not counting the blockage due to the boundary layer thickness, this would result in a thrust loss of about 3.5% for the tab case.

Fig. A6: The tabs were tried with the six lobed nozzle in an effort to increase mixing. That the tabs significantly alter the flow fields could be demonstrated readily by laser sheet flow visualization, as shown in this figure. The visualization technique is based on natural moisture condensation in the mixing layer where ambient air comes in contact with the cold core of the supersonic jet. Thus, the mixing layer region is illuminated by the laser sheet and seen in these pictures. It should be clear that four tabs, placed as shown in the sketch at the top of the right column, distort the jet differently compared to the no tab case.

Fig. A7: Similar flow visualization was conducted for various tab configurations, and the results are shown schematically in this figure. Tabs of two sizes were used: one had $w = 0.28$ cm representing approximately 0.8% area blockage, the other had $w = 0.18$ cm representing approximately 0.34% area blockage (w is defined in fig. A1). The mixing layer outline as seen at $x/D \approx 3$ are shown. Note that the tabs placed in the inner channel, as represented by the third case from the top, make little difference on the flow field. Also, a remarkable difference occurs depending on the size of the tabs. The tabs, on the outer four channels, are large in the fifth case from the top but are small in the sixth case from the top. This difference caused the different lateral spreading of the jet as shown.

Fig. A8: The mass flux variations obtained with the sixth case of fig. A7 are compared with the flux data shown before (fig. A4). For the sake of completeness, data obtained with both versions of the six lobed nozzle are shown in this figure. Recall that version #2 had outer chutes cut out so that there was some secondary flow due to natural entrainment. Clearly, this did not increase the mixing; in fact, the fluxes were even lower. The reason for this difference remained unclear. The tabs, however, certainly made an improvement. The thrust loss for the case with the tabs was discussed with fig. A5.

The rest of the data in Part A are for the P&W nozzle. Only flow field measurements could be conducted with this nozzle due to facility constraints. The large nozzle size, however, allowed adequate spatial resolution for the hot wire measurements.^{5,7} Key results, obtained by hot-wire as well as Pitot probe surveys, are presented in the following.

Fig. A9: The data shown in fig. A3 were for $M_j = 1.63$ which corresponded to a flow rate of about 3.6 kg/sec. Such a large flow rate caused high recirculation velocities in the limited volume of the test cell (approximately 12m x 6m x 6m). The flow noise was also too high to permit experimentation during normal working hours. Thus, a lower Mach number was chosen for further studies at supersonic conditions with the P&W nozzle.

Data, similar to those shown in fig. A3, for different tab configurations are shown in this figure at $M_j = 1.2$. The tab configurations are indicated by the insets in each figure. All tabs had the same size with $w = 1.1$ cm (fig. A1), which corresponded to an area blockage of about 0.7% per tab. Clearly, the effect of the tabs here is not as dramatic as observed with the circular jet. Nevertheless, some increase in the fluxes and changes in the jet cross sectional shape are caused by the tabs.

Fig. A10: Perhaps, of more significance is the effect of the tabs nearer to the nozzle exit which would be pertinent to the flow within the length of the ejector (typically a few equivalent diameters from the primary nozzle exit). Mach number distributions at $x/D = 2$, for the cases of fig. A9, are shown in this figure. The effect of the tabs in the near flow field is quite pronounced. The two and six tab cases make the jet cross section fuller which would be desirable with the ejector. Referring back to fig. A9, note that the eight tab configuration produced the largest increase in the mass flux downstream. However, this configuration may not be as effective with the ejector as the jet spreads mostly laterally at the upstream locations.

Fig. A11: Data corresponding to the cases of fig. A10, for $M_j = 0.31$, are shown in this figure. Whereas all the flow field data shown in the foregoing were obtained by Pitot probe traverses, the data in this and the rest of the figures in Part A were obtained by hot wire anemometry.

When compared to the data of fig. A10, the effect of the tabs can be found to be quite similar at supersonic and subsonic conditions. A similar observation was made earlier with axisymmetric nozzles, which led to the inference that compressibility has little to do with the primary effect of the tabs.¹ This is reassuring as the hot-wire measurements, conducted to determine the details of the flow field, could be carried out only at low subsonic conditions. It is likely that the inferences drawn from these data, e.g., about the vorticity dynamics, should be generally applicable at all Mach numbers.

Fig. A12: In this figure the streamwise evolution of the jet cross section for the no tab case is shown. The peaks and valleys in the velocity distribution are seen to smear out by $x/D = 2$.

Fig. A13: The variation of the mean velocity along the axis of the nozzle is shown in (a) for the four tab configurations. Corresponding variation measured with a circular nozzle is also shown for comparison. A faster decay of the jet velocity is indicated for the lobed nozzle, and this is affected differently by the different tab cases. A complete picture regarding the jet evolution can only be obtained by the detailed velocity distributions over the entire volume of the flow field. However, the centerline variations are easy to obtain and can be used for cursory assessment of the jet evolution. Such presentation is also customary in the literature and this prompted the inclusion of fig. A13. The corresponding centerline variations of turbulence intensities are shown in (b). Of note is the fact that the case with six tabs results in lower intensities and also a significant upstream shift of the second peak. The data shown in (a) also indicate that this case involves the fastest overall decay in the mean velocity.

Fig. A14: The evolution of streamwise vorticity, corresponding to the data of fig. A12, are shown in this figure. Each lobe produces a pair of counter-rotating streamwise vortices. Thus, initially there are eight pairs of such vortices. These, however, go through amalgamation and by $x/D = 2$ there are only four pairs left. A similar observation was also made earlier with circular jets; when too many tabs were used the vortices would undergo interactions and settle down to a fewer number. It is as if the jet cross section can accommodate only about two pairs of streamwise vortices and this number would be reached no matter how large the number is initially. The two resultant pairs of vortices, however, have been found to persist for a long distance downstream.⁵

Fig. A15: The effects of the different tab configurations on the streamwise vorticity distribution are shown in this figure. Clearly, there occurs a profound redistribution of the streamwise vorticity under the influence of the tabs.

Fig. A16: The sense of rotation of the streamwise vortex pairs observed with the P&W nozzle is explained in this figure. Each lobe produces a counter-rotating pair with the 'out flow' sense of rotation.⁷ These vortices are produced due to secondary flow within the nozzle.¹⁶ Placement of a tab produces a vortex pair with opposite sense, as shown in the inset on the left.¹ The vortices from the tab can be so strong that they simply overwhelm the naturally occurring vortices. However, the strength of the vortex pair depends on the tab size, a larger tab produces a stronger pair. Thus, since vorticity is diffusive, it might be expected that there exists a certain smaller size of the tab which will just null the naturally occurring vortices and there would be no resultant pair downstream.

When the tab is placed on the side of the nozzle, as shown in the inset on the lower right, it produces a vortex pair that augments the naturally occurring vortices occurring from the nearest lobes. For example the vortex on the right corner from the upper lobe has the same sign as the upper vortex produced by the tab. These two would amalgamate and produce a reinforced vortex. Such reinforcement of the natural vortices explains why just two tabs placed on the sides produced a remarkable effect on the flow field.

Fig. A17: Some of the detailed flow field data obtained together with the data of figs. A12 and A14 are documented in this figure. The longitudinal normal stress is shown in (a) while the two components of shear stresses are shown in (b) and (c). The contour interval is 0.02 in (a) and 0.001 in (b) and (c).

Fig. A18: Corresponding turbulent stress distributions for the tab cases of figs. A11 and A15 are shown in this figure. Not much further could be inferred on the dynamics of the flow field from the data of figs. A17 and A18. These data are included as they might be helpful in possible future analysis and computation of these flows.

Concluding remarks on Part A:

In terms of increasing jet mixing the effect of the tabs appears to be more pronounced than that of the lobes. The primary effect of the tabs is to produce streamwise vortex pairs while that of the lobes is to stretch the area of the mixing layer exposed to the ambient. The present data indicate that mixing increase due to the latter mechanism is not as efficient as that due to the dynamics of the vortex pairs. However, many lobe geometries are designed to produce strong streamwise vortices which might be just as effective as the tabs. Furthermore, the lobes of the present nozzle produced streamwise vortices through secondary flow, and thus, the relative roles of 'area increase' and 'streamwise vortex dynamics' in mixing enhancement remain far from completely clear. This issue as well as the dynamics of the streamwise vortex pairs responsible for increased mixing need to be addressed in the future.

The investigation also indicates that the jet flow field can accommodate only a few pairs of streamwise vortices. Thus, if too many vortex pairs are generated initially the vortices go through amalgamation or diffusion and settle to a fewer number. This occurs within a few equivalent diameters from the nozzle exit. Based on this evidence the usefulness of too many tabs or too many lobes might be questionable.

With the lobed nozzles, application of the tabs certainly alter the flow field. The effect is especially noticeable within the first few diameters from the nozzle exit. Based on the data obtained with the P&W nozzle it is thought that the cases involving two and six tabs have the best chance in producing positive effects when applied to the full scale experiment. Such an experiment with an actual Pratt & Whitney nozzle, together with the ejector and hot flow, is currently underway in the Nozzle Acoustic Test Rig (NATR).

PART B 'ACE NOZZLE' MODEL

Background: These experiments were conducted in the small jet facility with a simplified model of the ACE nozzle which is another configuration being considered for the HSCT aircraft (NASA Contract No. NAS3-25963). The nozzle model used in the present experiments approximately replicated only the primary flow. In a first set of experiments, a solid, pointed plug with 13° half-angle was used. Subsequently a 10° half-angle plug with rounded end and variable surface porosity was used. The effect of the tabs together with the different plugs was studied. Flow visualization, noise and thrust measurements were conducted. Because the tabs had to be applied to a narrow annulus in this case they had to be of smaller size compared to the size indicated in fig. A1(b). Two sets of delta tabs were used. In each set the area blockage to the flow was held constant while the number of tabs was varied. An objective of the investigation was to assess the effect of the number of tabs on thrust loss, mixing, and noise from the jet. The motivation came from an earlier observation with round nozzles which showed that, for a given area blockage, fewer larger tabs performed better than many smaller tabs. Key results are presented in the following.

Fig. B1: Pictures of the flow facility, nozzle and tabs are shown. The top picture shows the auxiliary plenum which is supplied with compressed air by four radial flexible tubes. The tubing seen in the middle is for measuring the plenum pressure. The plenum is mounted on linear bearings to enable thrust measurement with the help of a load cell.

The picture in the middle shows the nozzle fitted with the pointed plug. The picture at the bottom shows the five tab discs. The tab discs were installed with a retainer and screws. The

tab discs were wire-cut from shim stock with thicknesses ranging from 0.0076 cm to 0.025 cm depending on the sizes of the tabs. The tabs were bent approximately 45° with a suitable die. The tab designations are indicated in the figure and explained in the nomenclature. The base width of the tabs for the five cases, reading from left to right in the figure, is 0.264, 0.188, 0.137, 0.137, and 0.066 cm. The last one, the 24_1% case, is approximately comparable in scale to the hardware used in an earlier Boeing experiment.

Fig. B2: The nozzle fitted with the pointed plug is shown schematically in (a). The nozzle converged from 3.81 cm dia to 1.91 cm dia then diverged and converged over the centerbody (plug) terminating with a diameter of 2.1 cm. The shape and location of the plug was such that the flow converged throughout the annular passage. Thus, all the supersonic cases involved underexpanded flows. The annulus at the exit was measured with filler gages and found to be a maximum of 0.292 cm on one side and a minimum of 0.279 cm on the other; the equivalent diameter, D was 1.44 cm. The outer lip of the nozzle was not sharp and the thickness (i.e., the 'end wall') was left to allow easy installation of the tab discs.

The geometry of the 10° half-angle, rounded plug is shown in (b). The porous part of the plug is interchangeable. The axial location of the plug was adjusted so that the equivalent diameter of the annular exit was about the same as with the pointed plug. The porous plug notations have been explained in the nomenclature section.

Fig. B3: This figure shows the laser sheet illuminated cross section of the jet about 0.6 cm downstream from the tip of the pointed plug. As stated earlier, the visualization shows the mixing layer region as the bright area. The asymmetry in the jet cross section is believed to be a result of the camera angle and the three struts holding the plug (fig. B2a). It can be seen that some of the tab configurations clearly increased the jet spreading. More spreading occurred with the cases involving lesser number of tabs. The 24 tab case in both sizes (1% and 4% blockages) produced minimal effect.

The rest of the results presented in the following are obtained with the 10° rounded plugs.

Fig. B4: Sample flow visualization pictures with the rounded plugs are shown in this figure. (These pictures were obtained at a different time and, in contrast to fig. B3, the flow is from left to right in these pictures.) Essentially the same effect of the tabs was observed. The effect of the porosity of the plug was not discernible from these pictures.

Fig. B5: Schlieren photographs are shown for the flow field around the plug. The shock/expansion structure around the plug can be seen for the no tab cases. The structures appear to be somewhat diffused with the 5.5%H plug compared to the solid plug case. Again, the difference

in the upper and lower halves in these pictures is believed to be due to the asymmetry introduced by the struts holding the plug. The effect of the tabs in either plug case is profound, as seen in the lower two pictures. The discrete shock/expansion structure appears to be weakened and diffused significantly.

The effect of 6 and 24 tabs, with the solid plug, is shown in fig. B5(b). The effect of 6 tabs is similar to that of 12 tabs. However, here some discrete shock structures with reduced spacings can be discerned. With 24 tabs the shock structure approximately returns to the structure seen for the no tab case.

Thrust Loss:

Fig. B6: This figure shows comparison of thrust (T, Newtons) vs. NPR for the four porous plug cases with that for the solid plug case. All cases are seen to involve significantly lower thrust from the 'ideal'. This is likely to be due to substantial boundary layer thickness relative to the annulus dimension. 'Ideal' thrust implies isentropic calculation assuming uniform flow at the nozzle exit (zero boundary layer thickness). The thrust variations are similar for all plug cases. At NPR = 4.47, the thrust loss from 'ideal' is found to be 5.7% for the 3.6%H case and 6.9% for the 10%S case, the others being close to 6%.

Note that this and the rest of the figures in the report are presented in their original computer printout forms. The tables on the right may be ignored. However, a curious reader might find some more information from these. For example, the percent thrust loss at NPR = 4.47 is listed in the upper table. In the lower table, '%blkg' represents (two times the) percent flow blockage computed from measurements of actual mass flow, the nozzle pressure ratio and the nozzle exit area; 'cd0' represents orifice meter discharge coefficient obtained from calibration with a circular nozzle; 'cf1' and 'cf2' are coefficients of performance described in the nomenclature.

Fig. B7: The effect of the end hole size (see fig. B2b) on thrust is shown. The hole diameters in inches are indicated. The effect, for the present case, is negligible.

Fig. B8: Thrust versus NPR is shown for the indicated tab cases. All three tab configurations involve thrust loss, the least is with the 6_4% tab case.

Fig. B9: Thrust coefficient vs. NPR are shown corresponding to the data of fig. B8. Here, the six tab case exhibits the least performance loss. With the pointed plug, twelve tabs performed best (data are not shown for brevity). However, uncertainty in these data are large, estimated to be equal to one ordinate division, due mainly to error in the mass flow measurement.

Fig. B10: While the data in fig. B9 were taken with the solid plug, this figure shows corresponding data taken with the 5.5%H plug. Here, the loss due to the three tab configurations is practically identical.

Noise data:

Far field noise was measured at a distance of 67D, and an angular location of 110° from the downstream axis of the jet. Spectral analysis was done with an analyzer (Nicolet 660B) with bandwidth $\Delta f = 250$ Hz. It should be noted that the test cell was only semi-anechoic and thus the amplitudes may be contaminated especially at the lower frequency end. However, the comparisons for the relative effects of the tabs or the porous plugs should be valid.

Fig. B11: Spectra for the four porous plug cases are compared with that for the solid plug case. Successive pairs of curves are staggered by one major ordinate division; the ordinate shown pertains to the pair at the bottom. In (a), at the higher NPR, the porous plugs are seen to make little difference in the noise spectra compared to the spectrum for the solid plug case. This is not so at the lower NPR in (b), where all porous plugs are seen to produce additional noise!

Again, the notations and tables on the right of these figures may be ignored. But additional information can be obtained; the list in the table pertains to the spectra traces starting from the bottom. For example, in (b), rec 307 is the solid curve and rec 306 is the dashed curve in the bottom pair. The fully expanded Mach number (M_j) is indicated in the second column; 'scr_f' represents frequency (kHz) of the highest peak in the spectra, 'scr_a' represents the corresponding amplitude in dB, and 'oaspl' represents overall sound pressure level in dB.

Fig. B12: Data for three tab configurations together with the 5.5%H plug are compared with data for the no-tab, solid plug case. The 12_4% tab results in the most overall noise reduction, at both NPR.

Fig. B13: Data for the porous plug and the solid plug are compared. Together with the tabs, the porous plug results in slightly lower amplitudes at the higher NPR in (a). The comparison is much more favorable for the porous plug at the lower NPR in (b).

Fig. B14: Data for the porous plug and the solid plug, without tabs, are compared in (a) at four values of NPR. For some unknown reason (and there are many in this complex problem!), the solid plug produces less noise at NPR = 3.5 (see also fig. B11b). At other values of NPR, the difference in the data is little.

The data in (b) show that the slot plug (dashed curves) produces additional noise compared to the plug with holes (solid curves), especially at lower NPR.

Fig. B15: The effect of 12_4% tab case (with the solid plug) is compared with the no tab case at four values of NPR. At higher NPR, the reduction in noise at lower frequencies is accompanied by some increase at higher frequencies.

Fig. B16: The effects of the 12_4% tab with the solid plug (dashed curves) and the 5.5%H plug (solid curves) are compared at four values of NPR. The porous plug yields some additional noise benefit.

Fig. 17: Finally, the noise spectra for the ACE nozzle, with and without the tabs, are shown in comparison to the spectra for the six lobed nozzle (Part A) and for an elliptic nozzle. The two pairs of spectra at the top show comparison between the six lobed nozzle and the 3:1 elliptic nozzle, on both minor and major axis planes. As mentioned with fig. A4, no screech is observed for the six lobed nozzle. The ACE nozzle without tabs can be seen to have screech components. The pair of spectra at the bottom shows that the ACE nozzle with the 12_4% tabs produces the least noise among the cases considered in this figure.

Concluding remarks on Part B:

The following inferences are made:

- (1) Jet spreading is undoubtedly more with fewer larger tabs.
- (2) Tab effect on noise far outweighs the effect produced by the porous plugs.
- (3) Together with the tabs, the porous plugs produce additional noise benefit over the solid plug.
- (4) The 12_4% tab together with the 5.5% porous plug produced the least noise.

The reason why many small tabs, as compared to few larger tabs, do not work well even with a simple round nozzle is not completely clear. It is possible that, since a tab does not work well if it is submerged in the boundary layer, an increasing ineffectiveness with smaller size may explain this trend. For a given total area blockage, or for a given size of each tab, there should exist an optimum number which would work best. For about 1.7% area blockage each, four delta tabs with a simple round nozzle increased the jet spreading the most; increasing the number of tabs caused a reversal in the effect. For smaller size tabs the optimum number can be expected to be larger.

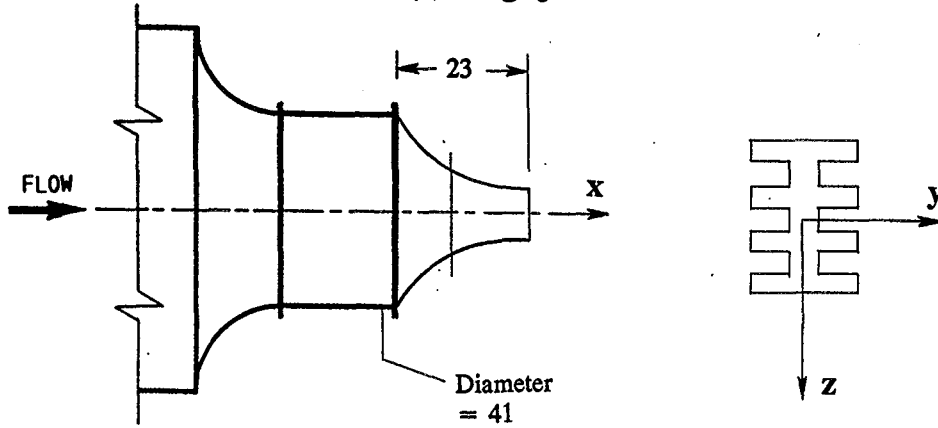
In the ACE nozzle model it is apparent that the boundary layer thicknesses are large relative to the width of the annulus. This might be the reason why the smallest size tabs did not make a noticeable effect on the flow field. In the full scale nozzle the boundary layer can be expected to be much thinner relative to the annulus width. This may be why a scaled up tab configuration corresponding to the 24_1% case was quite effective in an earlier Boeing experiment. However, based on the present results, six to twelve delta tabs may be expected to work even better. This ought to be tried in the full scale experiment. It is also desirable that for a given number of the tabs, the total area blockage be varied, perhaps, ranging from 0.5% to 6%, to find the optimum effect.

References:

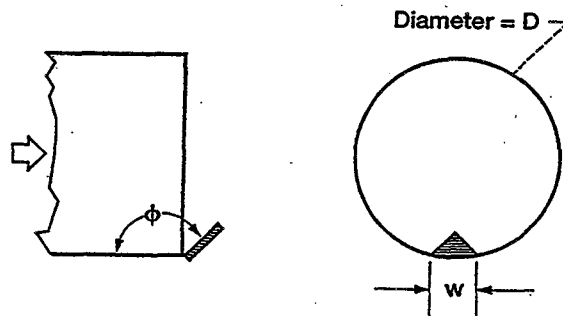
- ¹Zaman K.B.M.Q., Reeder M.F., and Samimy M., 1994, "Control of an axisymmetric jet using vortex generators", *Physics of Fluids A*, 6 (2), pp. 778-793.
- ²Ahuja K. K. and Brown W. H., 1989, "Shear flow control by mechanical tabs", *AIAA Paper* No. 89-0994.
- ³Samimy M., Zaman K.B.M.Q. and Reeder M.F., "Effect of tabs at the nozzle lip on the flow and noise field of an axisymmetric jet", *AIAA J.*, 31(4), pp. 609-619 (1993).
- ⁴Reeder, M.F. and Zaman, K.B.M.Q., "The impact of 'tab' location relative to the nozzle exit on jet distortion", 30th Joint Prop Conf., Indianapolis, IN, July 27-29, 1994, *AIAA 94-3385*.
- ⁵Zaman, K.B.M.Q., 1993, "Streamwise vorticity generation and mixing enhancement in free jets by 'delta-tabs'", AIAA Shear Flow Conference, July 6-9, 1993, *AIAA 93-3253* (NASA TM 106235).
- ⁶Zaman K.B.M.Q., 1994, "Effect of 'delta tabs' on mixing and axis switching in jets from asymmetric nozzles" *AIAA Paper* 94-0186, Aerospace Sciences Meeting, Reno, NV, Jan.
- ⁷Zaman K.B.M.Q., 1995, "Axis switching and spreading of an axisymmetric jet -- role of vorticity dynamics", *AIAA Paper* 95-0889, Aerospace Sciences Meeting, Reno, NV, Jan., 1995.
- ⁸Tanna H.K., "An Experimental Study of Jet Noise, Part II: Shock Associated Noise", *J. Sound & Vib.* vol. 50, 429-444 (1977).
- ⁹Dahl M.D. and Morris P.J., "Supersonic jet noise reductions predicted with increased jet spreading rate", submitted for ASME/JSME Fluids Engineering Conf., Hilton Head, SC, Aug. 13-18, 1995.
- ¹⁰ Kobayashi, H., Oinuma, H., Sawamura, T. and Outa, E., "Effects of tab size on supersonic underexpanded cold and heated jet noise suppression and jet thrust loss", *AIAA Aeroacoustics Conf. (93-4348)*, Long Beach, CA, Oct. 1993.
- ¹¹ Wolter J.D. and Jones C.W., "Pratt & Whitney two dimensional HSR nozzle test in the NASA Lewis 9-by 15-foot low speed wind tunnel: aerodynamic results", *Proc., First NASA/Industry HSR Program Nozzle Symposium*, Nov 17-19, 1992.
- ¹²Crow S.C. and Champagne F.H., "Orderly structures in jet turbulence", *J. Fluid Mech.*, 48, 547-591 (1971).
- ¹³Norum T.D., "Screech suppression in supersonic jets", *AIAA J.*, 21, pp. 235-240 (1983).
- ¹⁴Ho, C.-M. and Gutmark, E., 1987, "Vortex induction and mass entrainment in a small-aspect-ratio elliptic jet", *J. Fluid Mech.*, vol. 179, pp. 383-405.
- ¹⁵Hussain F. and Husain H.S., 1989, "Elliptic jets. Part 1. Characteristics of unexcited and excited jets", *J. Fluid Mech.*, 208, pp. 257-320.
- ¹⁶Bradshaw, P., "Turbulent secondary flows", *Ann. Rev. Fluid Mech.*, 19, pp. 53-74, (1987).

EXPERIMENTAL FACILITY

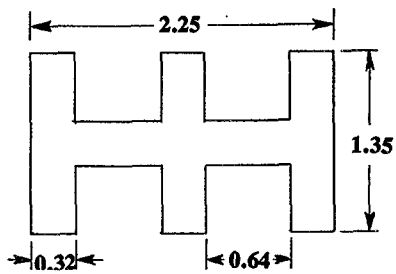
(a) Large jet and coordinates



(b) delta tab



(c) Six lobed nozzle



(d) Eight lobed (P&W) nozzle

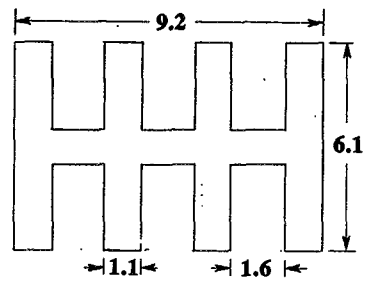


FIG. A1

EIGHT LOBED 'P & W' NOZZLE MODEL

NASA
C-94-24239



NASA
C-99-05748

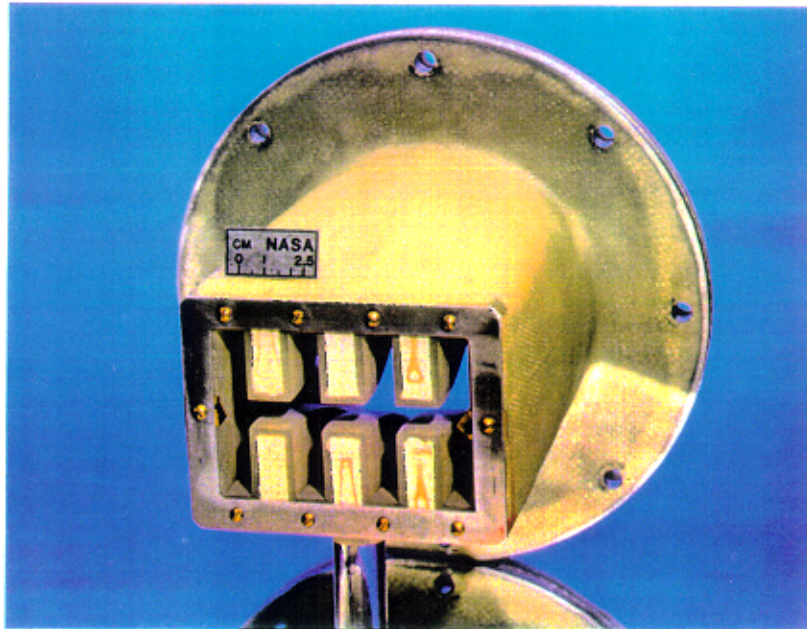


FIG. A2

M-CONTOURS; $x/D = 14$, $M_j = 1.63$

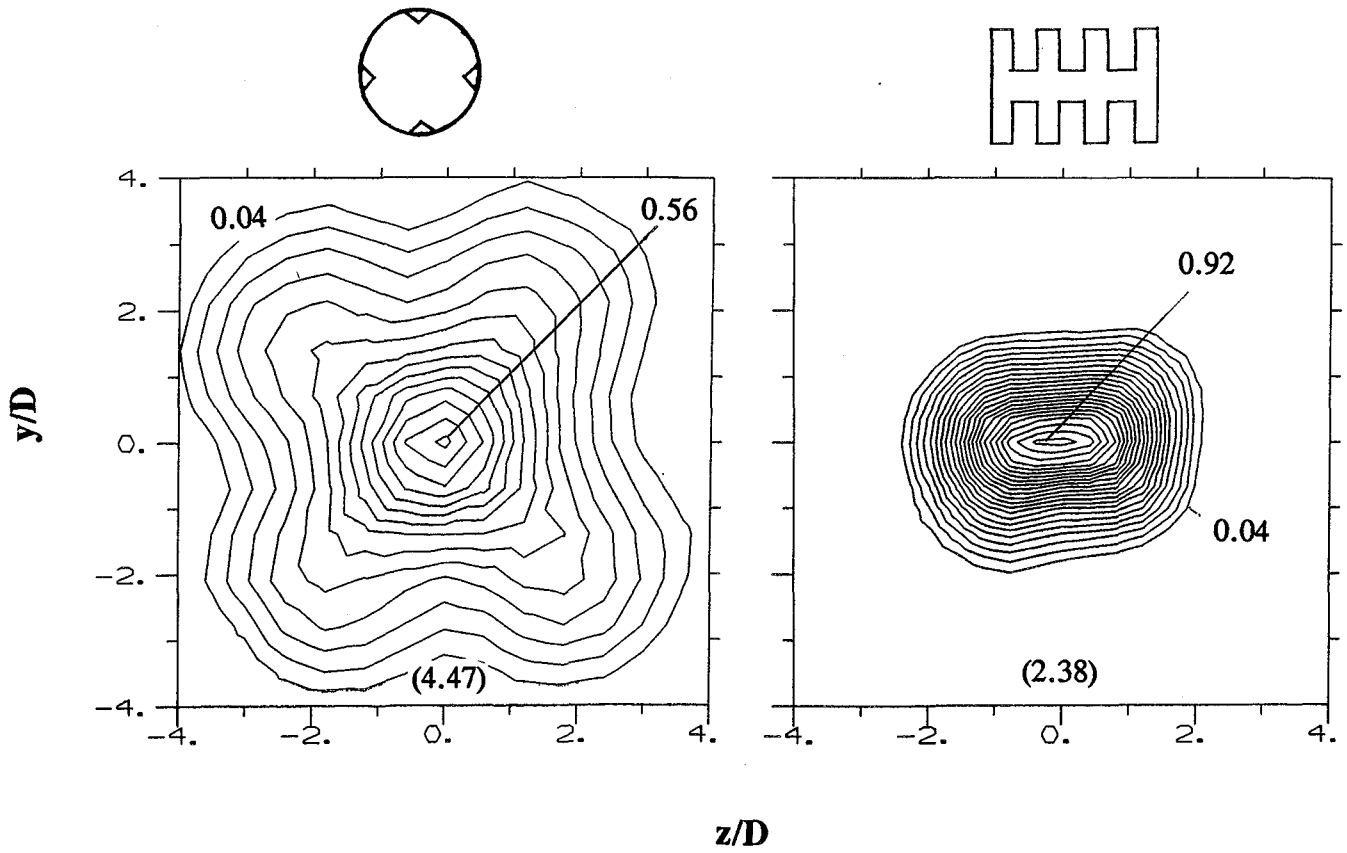


FIG. A3

THRUST VERSUS NPR

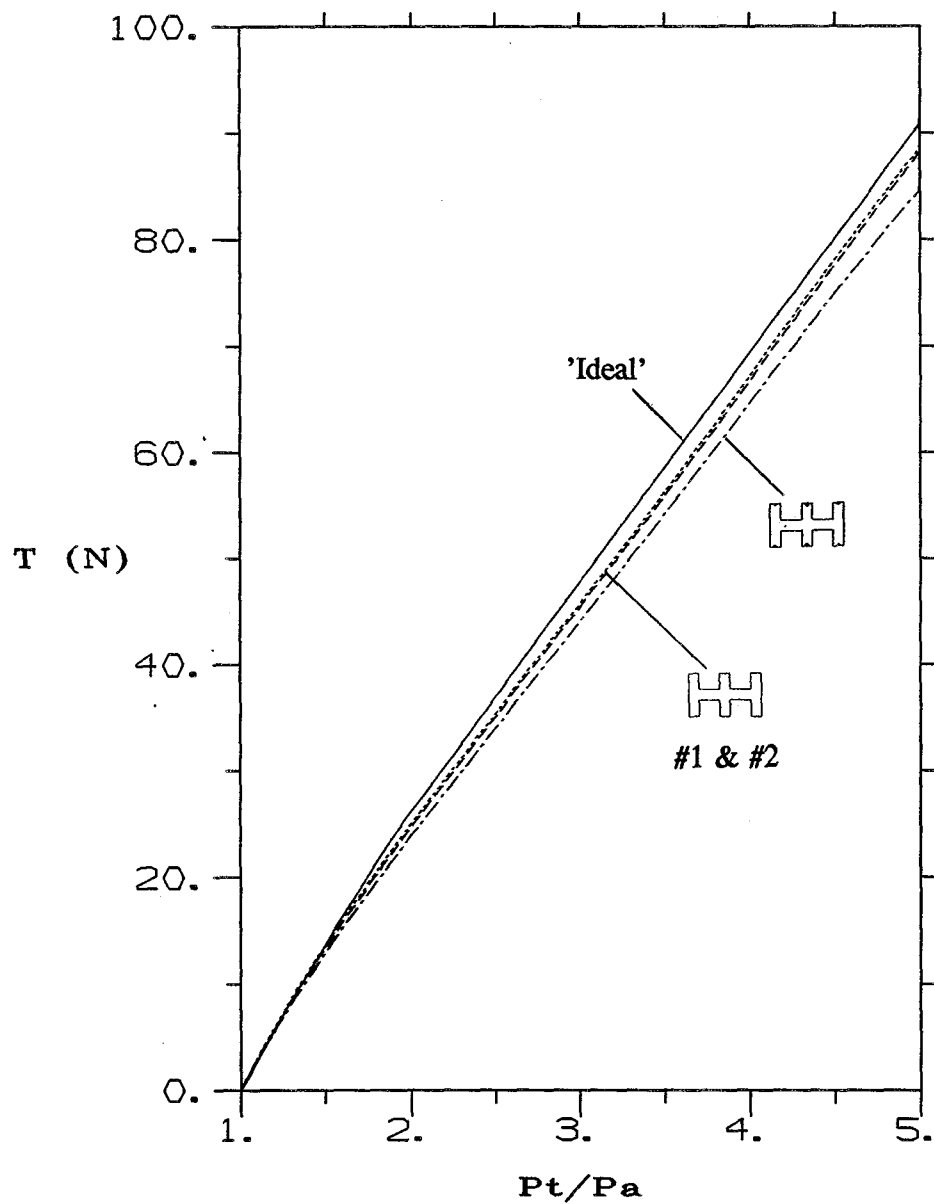


FIG. A5

LASER SHEET FLOW VISUALIZATION, $M_j = 1.63$

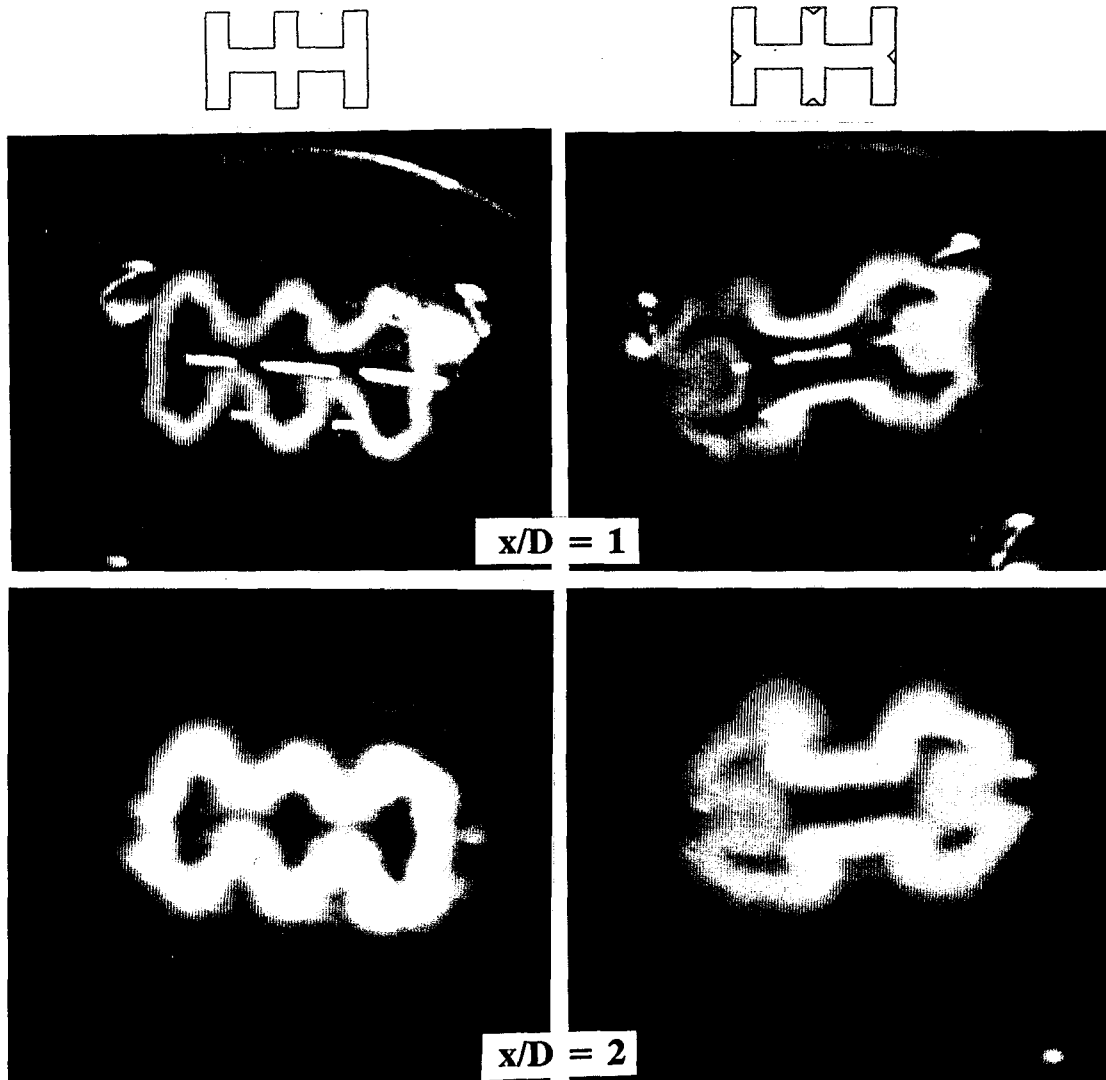


FIG. A6

**SKETCHES OF JET DISTORTION AT $x/D \sim 3$
FOR INDICATED TAB CONFIGURATIONS, $M_i = 1.63$**

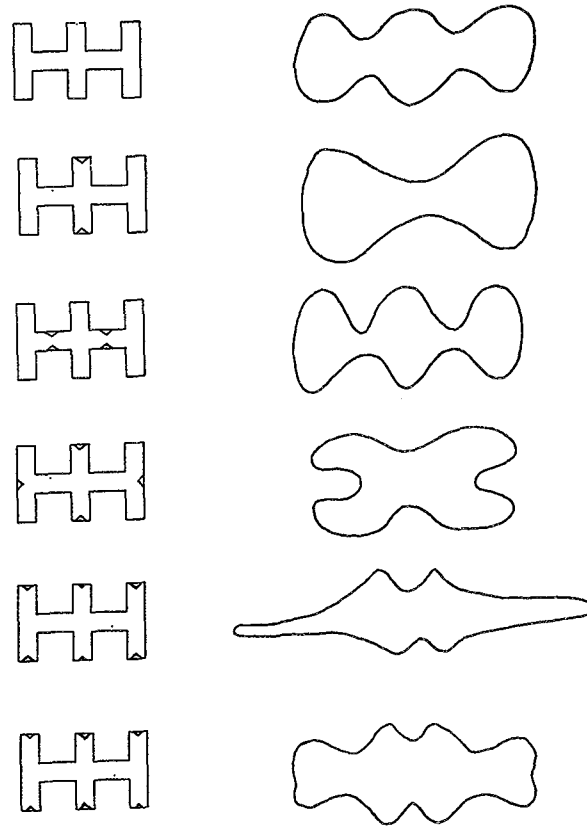


FIG. A7

NORMALIZED MASS FLUX VERSUS x/D , $M_j = 1.63$

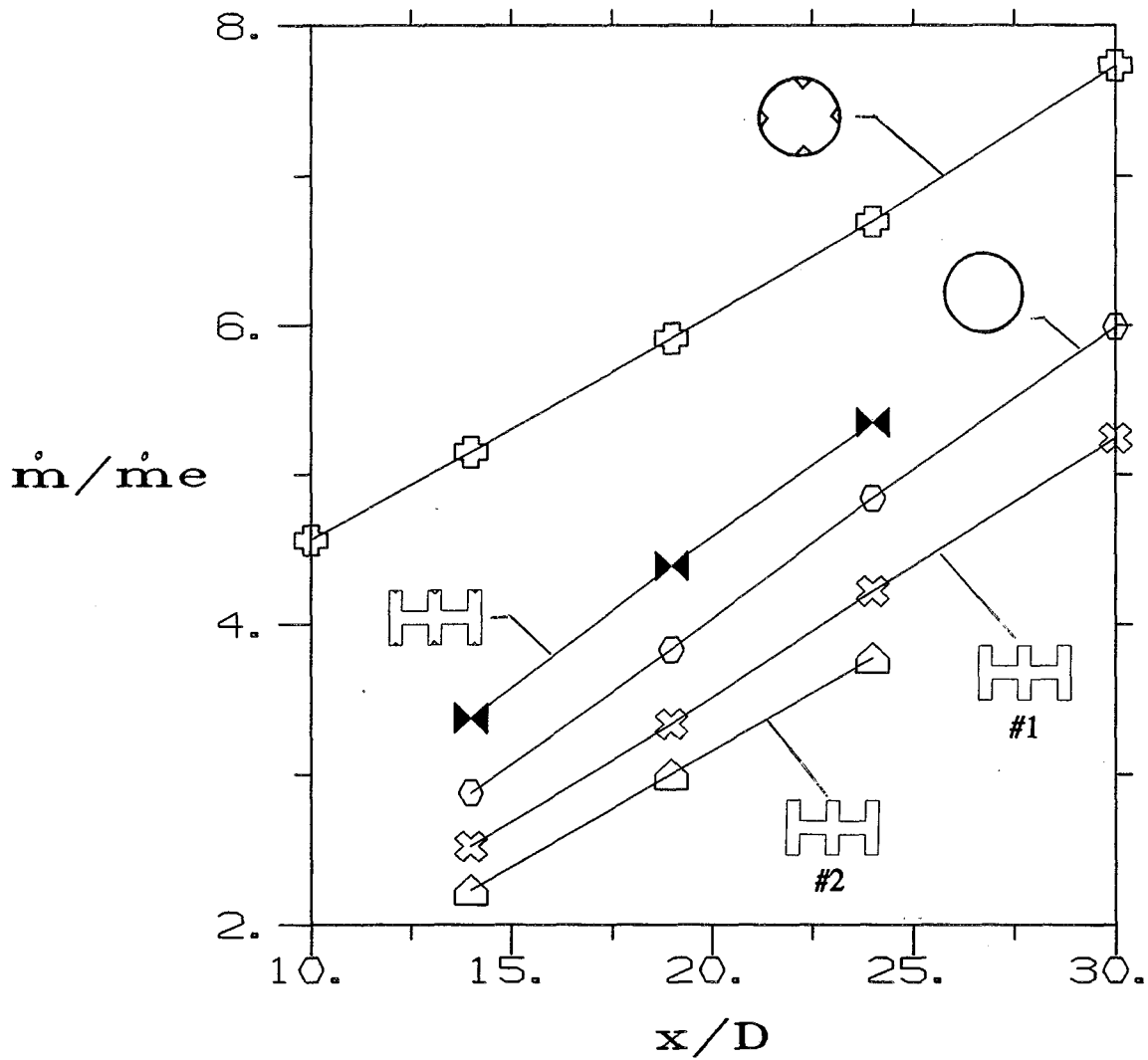


FIG. A8

M-CONTOURS; $x/D = 14$, $M_j = 1.2$

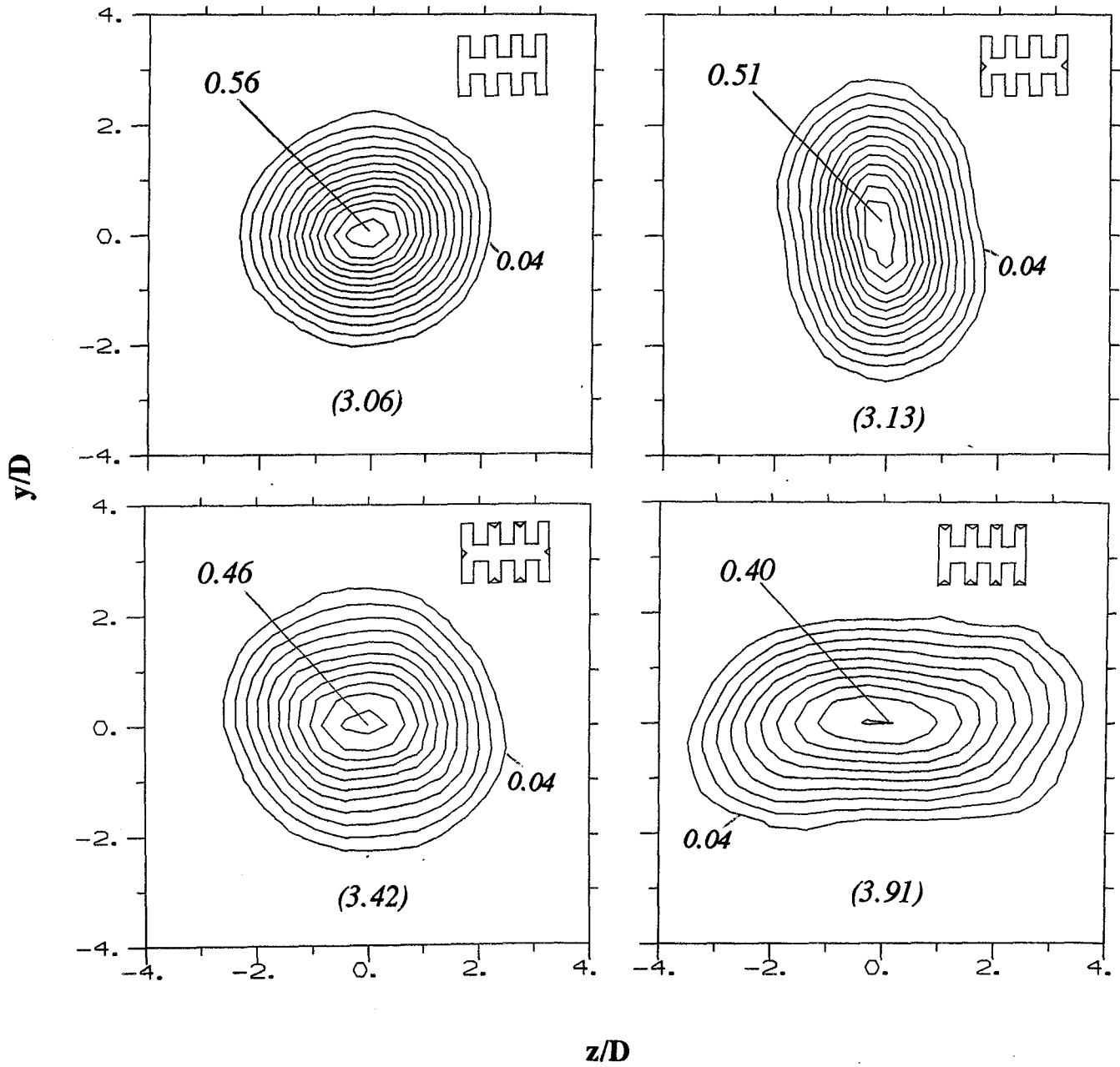


FIG. A9

M-CONTOURS; $x/D = 2$, $M_j = 1.2$

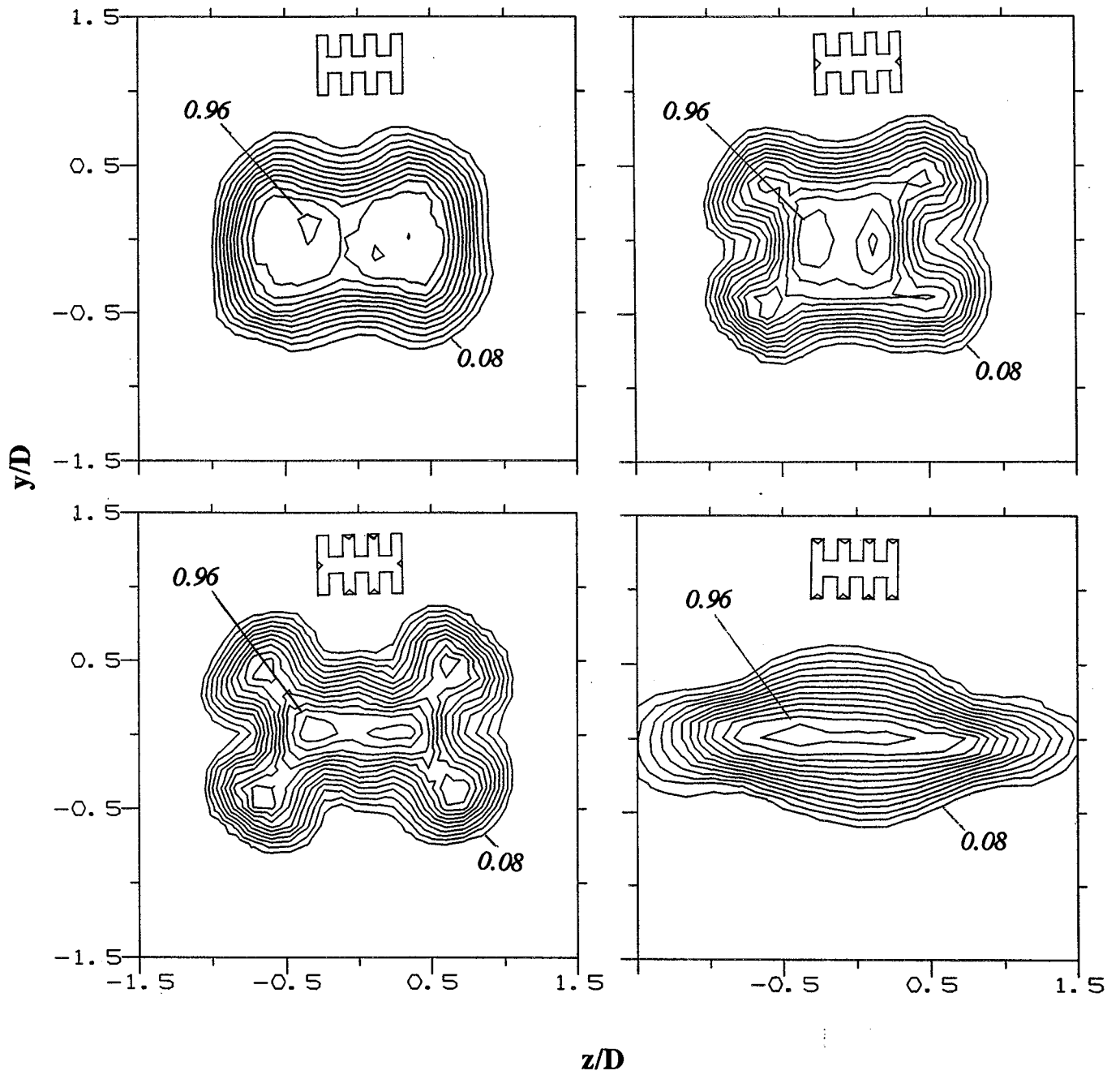


FIG. A10

U/U_j -CONTOURS; $x/D = 2, M_j = 0.31$

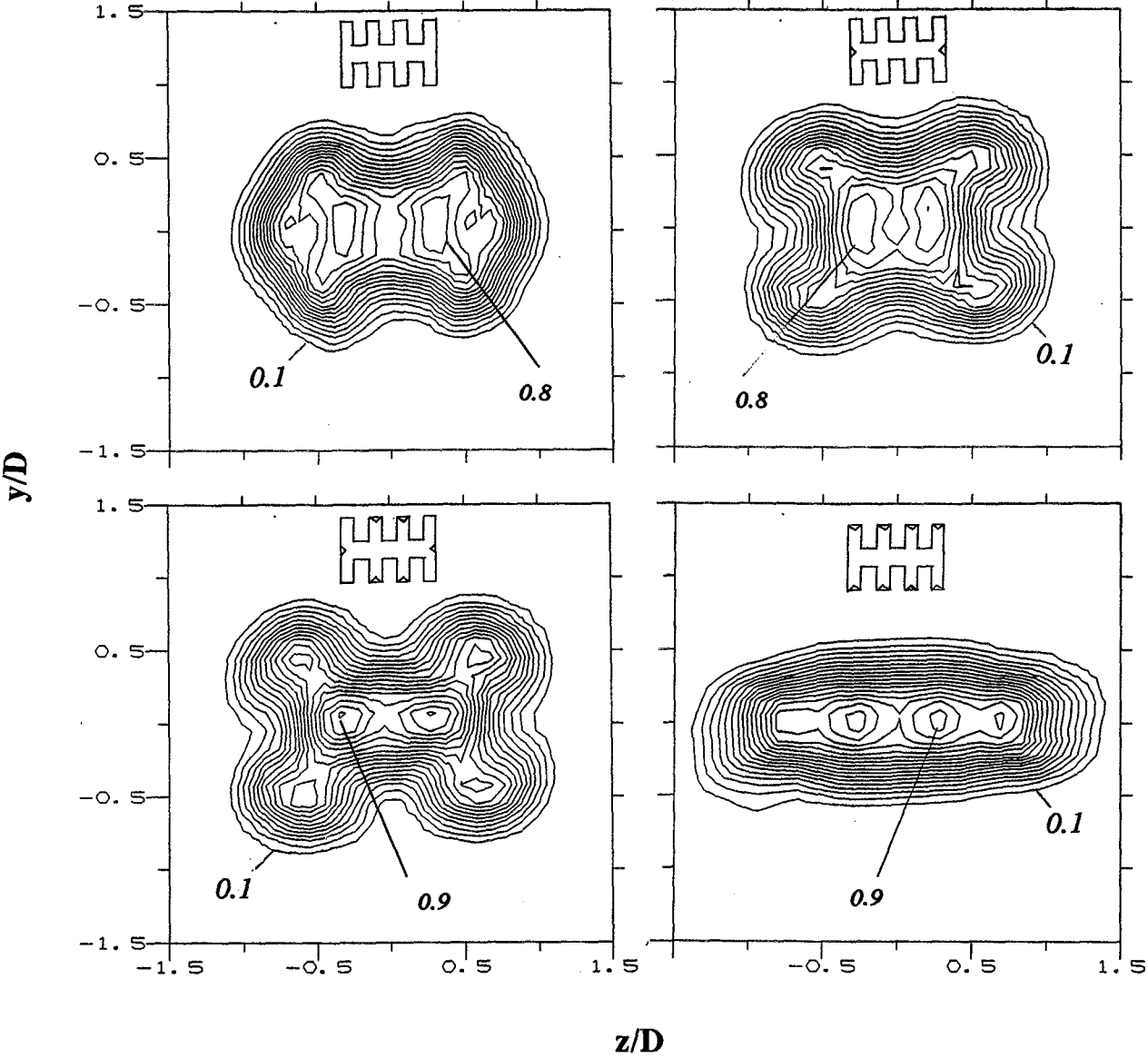


FIG. A11

U/U_j -CONTOURS; FOR INDICATED x/D , $M_j = 0.31$

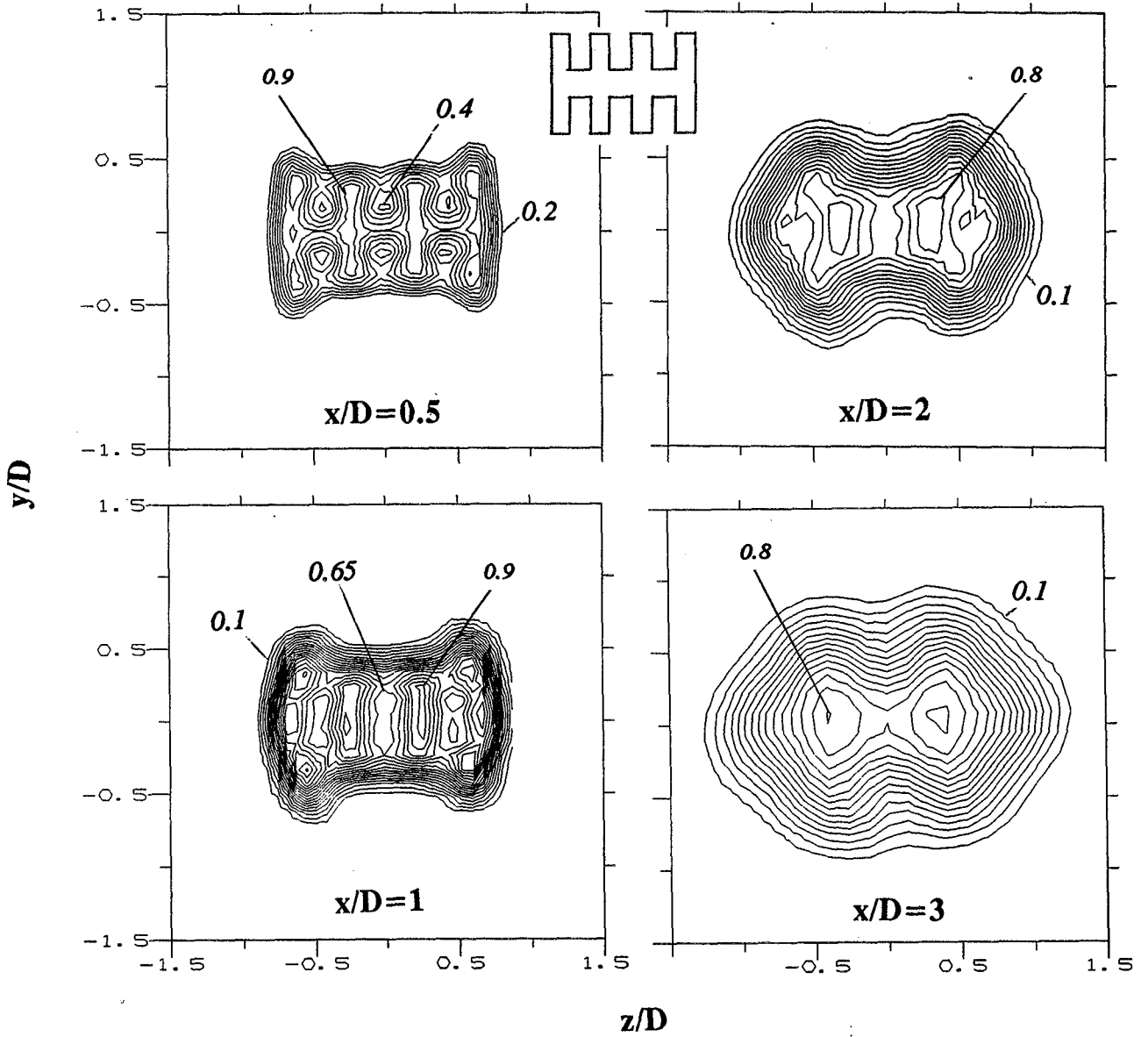


FIG. A12

CENTERLINE MEAN VELOCITY VARIATION, $M_j = 0.31$

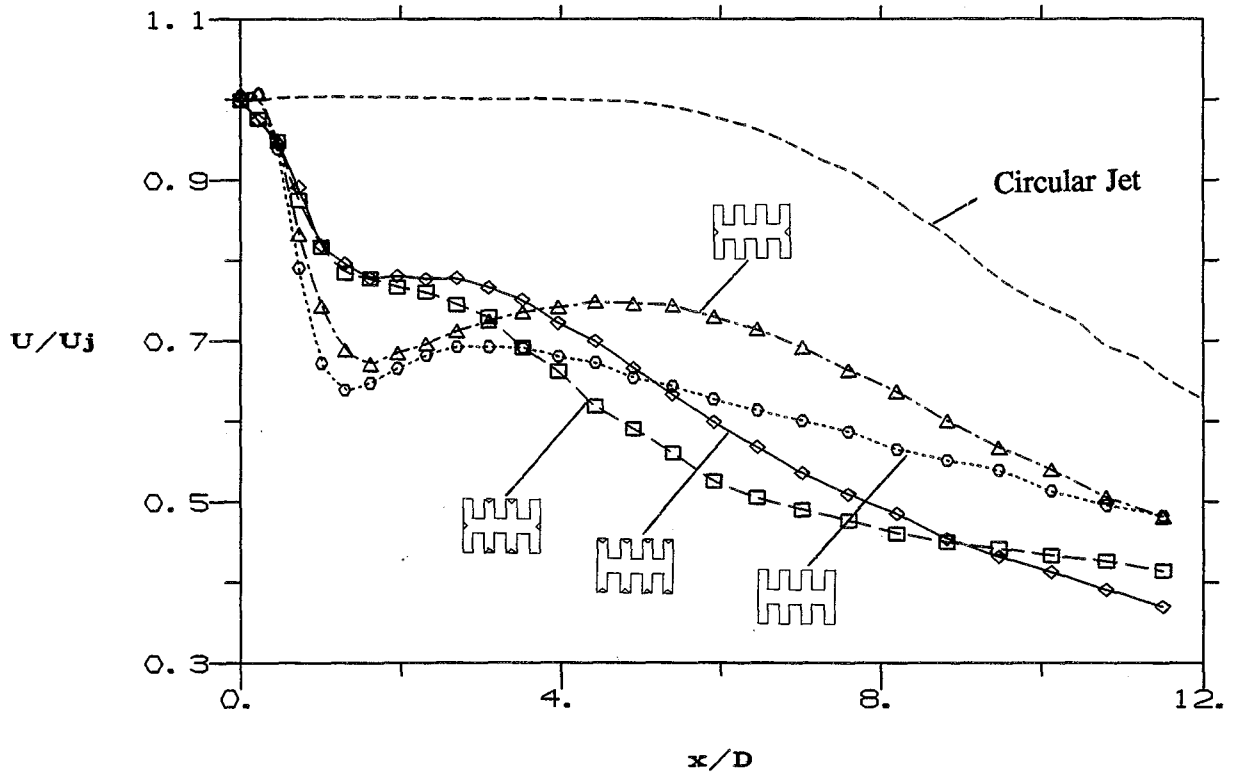


FIG. A13(a)

CENTERLINE TURBULENCE INTENSITY VARIATION

$M_j = 0.31$

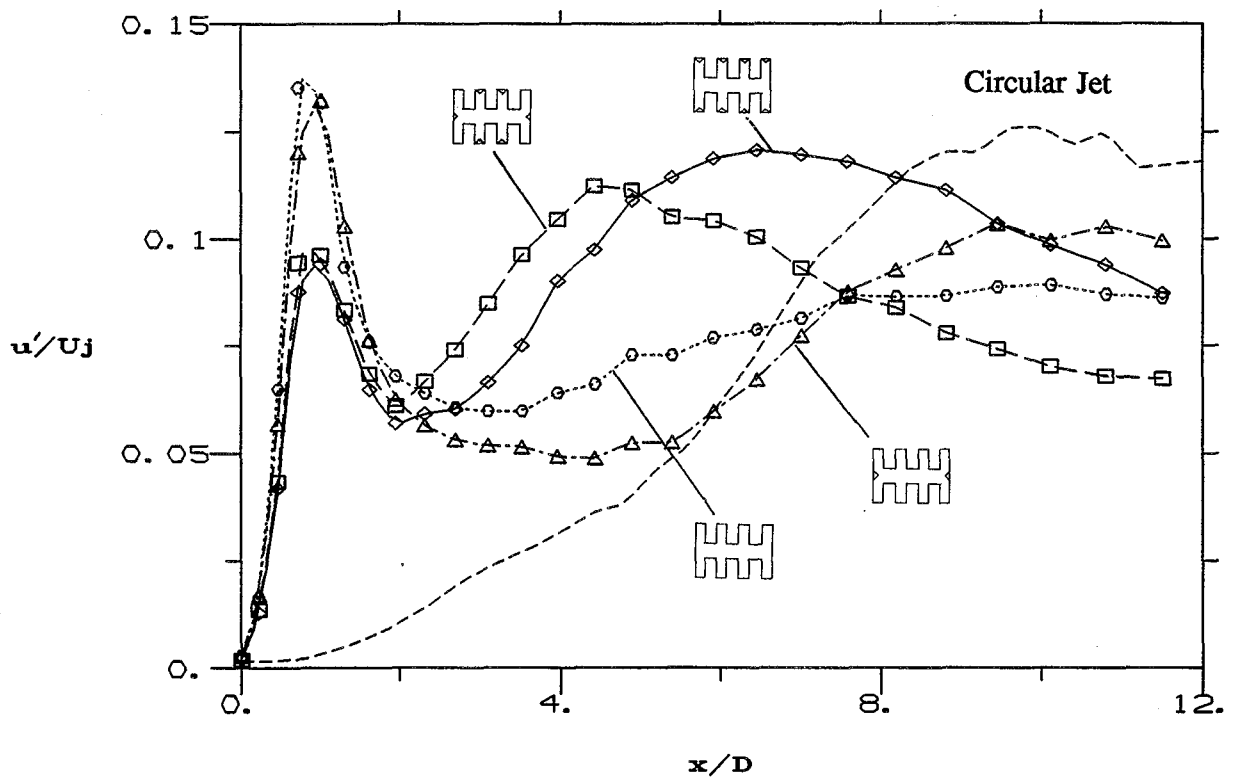


FIG. A13(b)

$\omega_x D/U_j$ -CONTOURS; FOR INDICATED x/D , $M_j = 0.31$

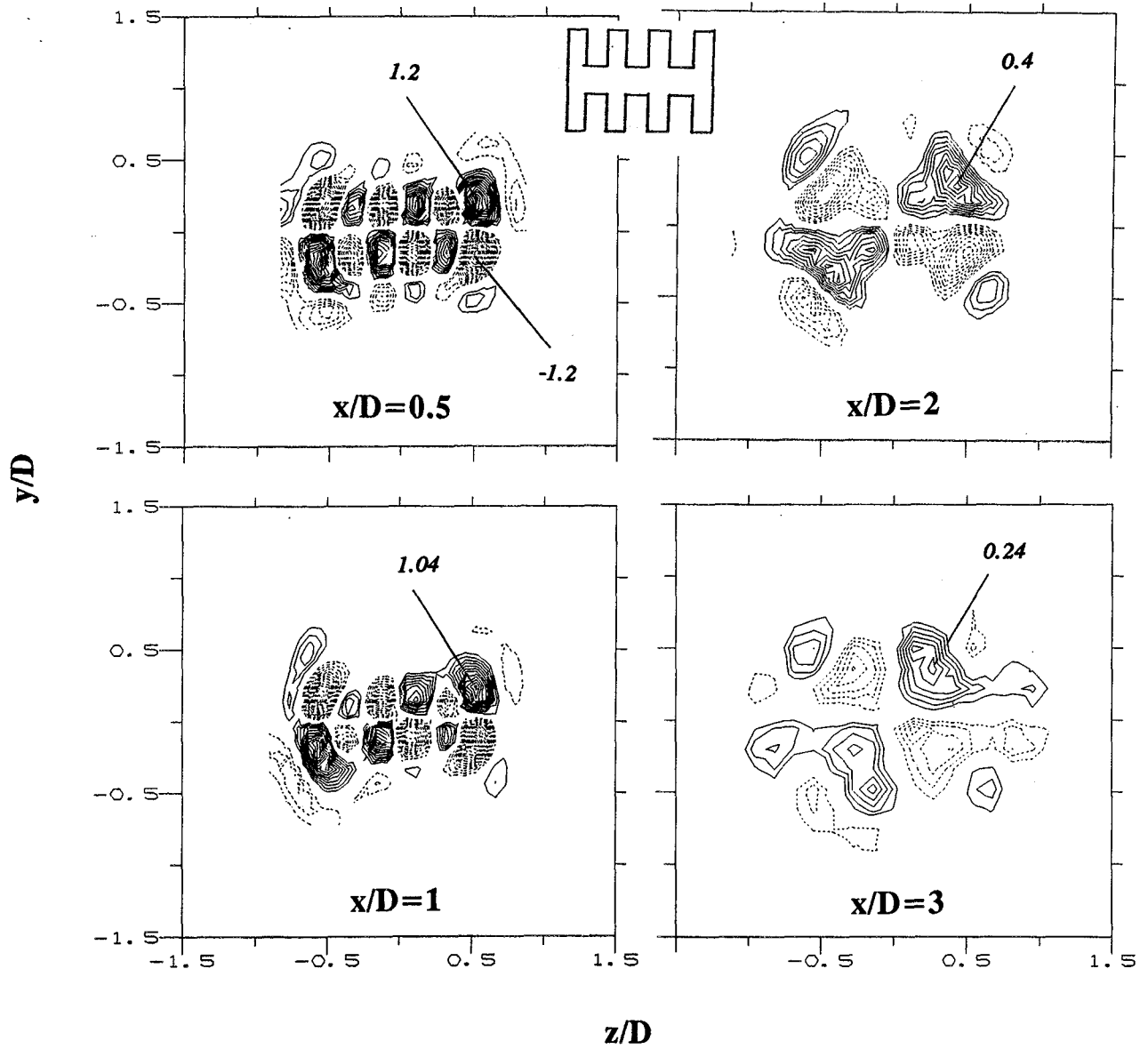


FIG. A14

$\omega_x D/U_j$ -CONTOURS; $x/D = 2, M_j = 0.31$

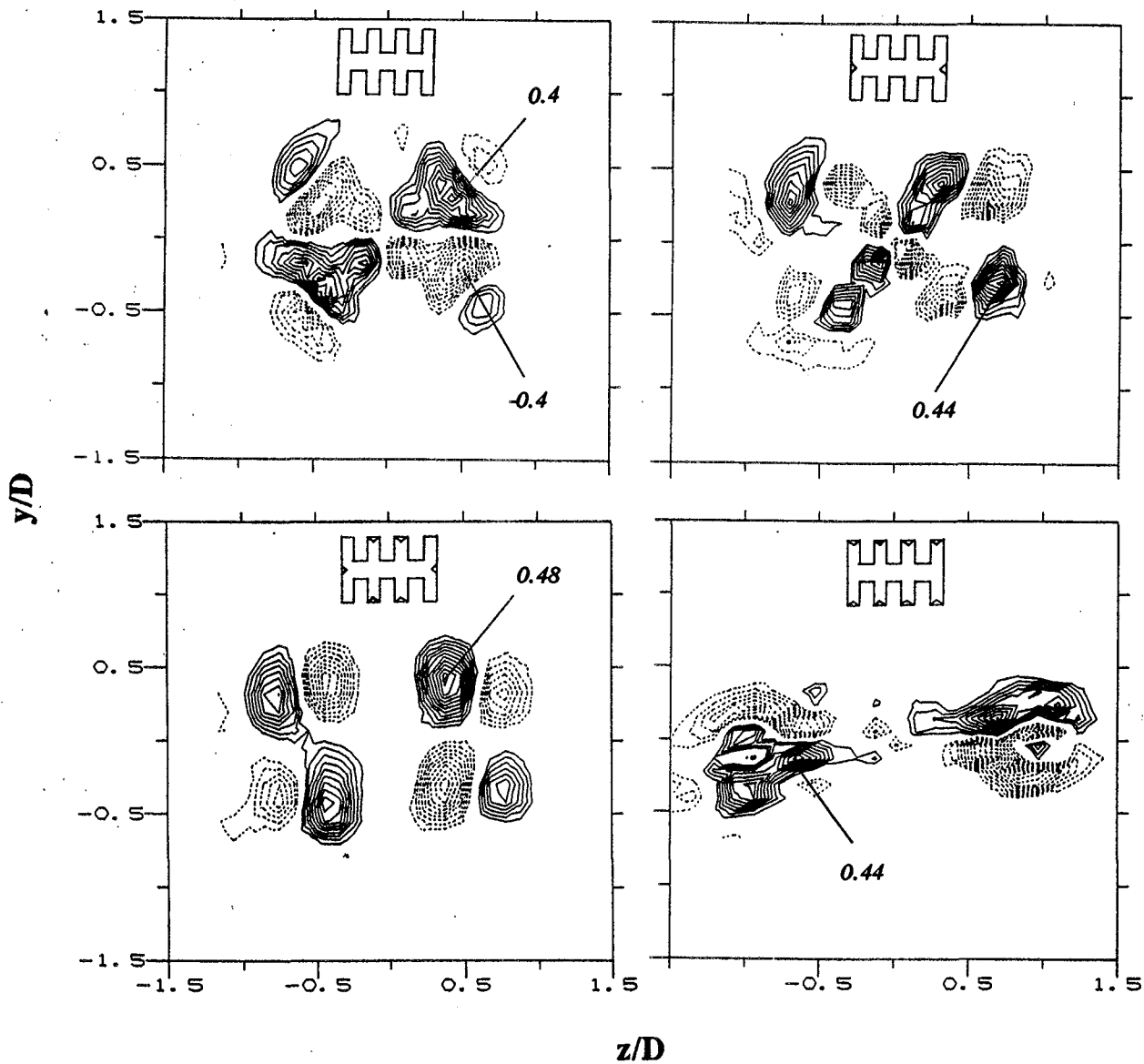


FIG. A15

SKETCH OF STREAMWISE VORTICITY DISTRIBUTIONS

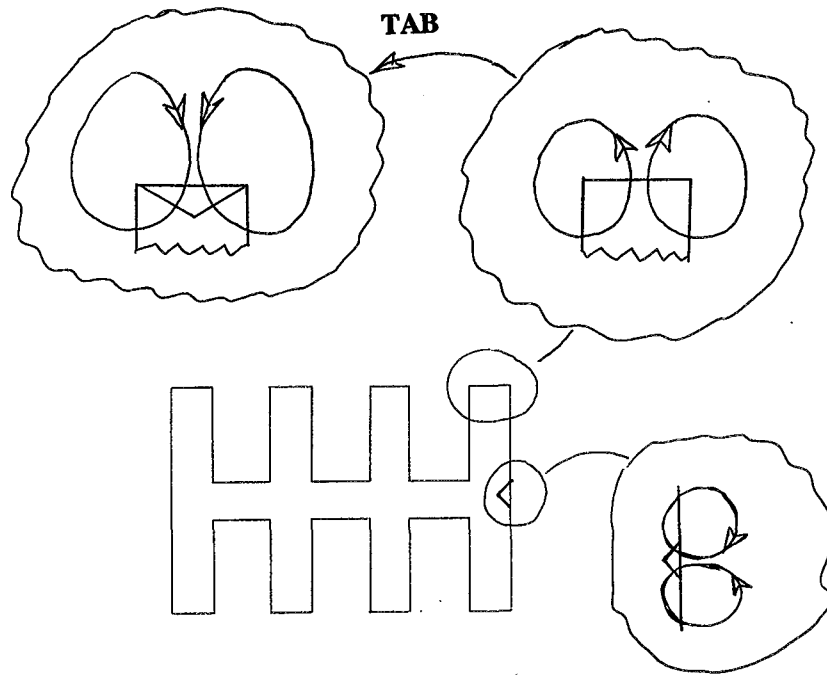


FIG. A16

u'/U_j -CONTOURS; FOR INDICATED x/D , $M_j = 0.31$

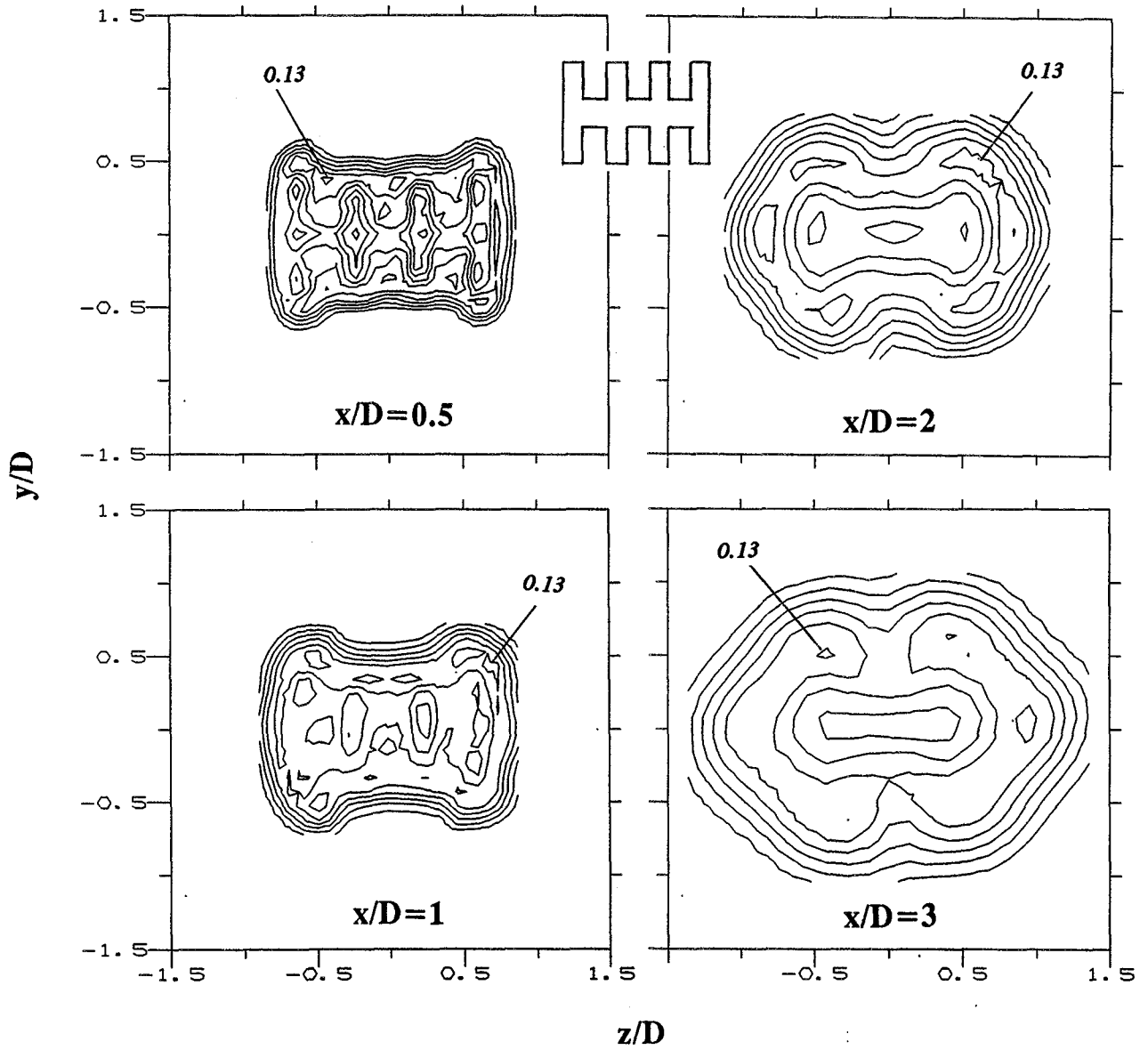


FIG. A17(a)

\overline{uv}/U_j^2 -CONTOURS; FOR INDICATED x/D , $M_j = 0.31$

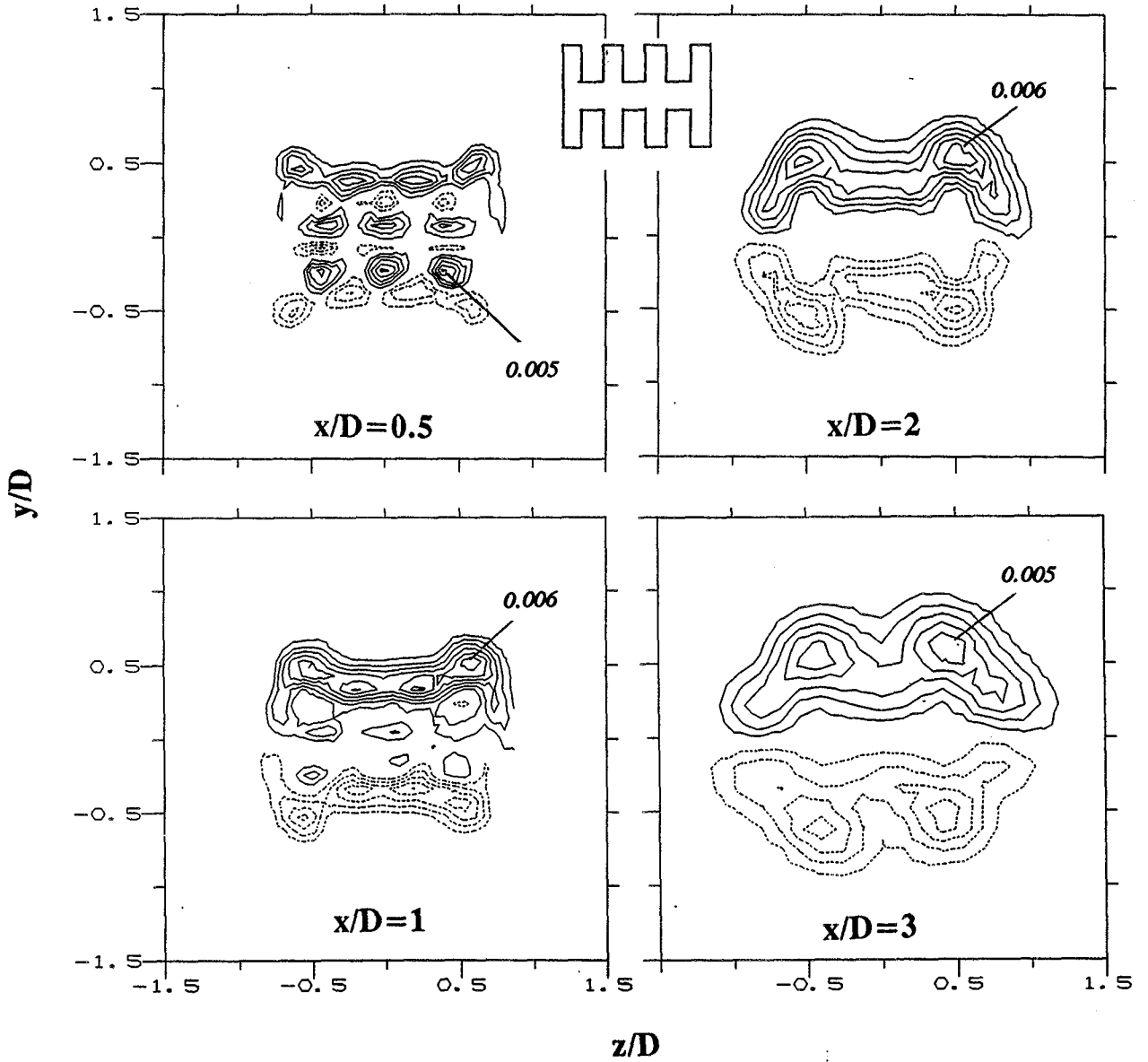


FIG. A17(b)

\overline{uw}/U_j^2 -CONTOURS; FOR INDICATED x/D , $M_j = 0.31$

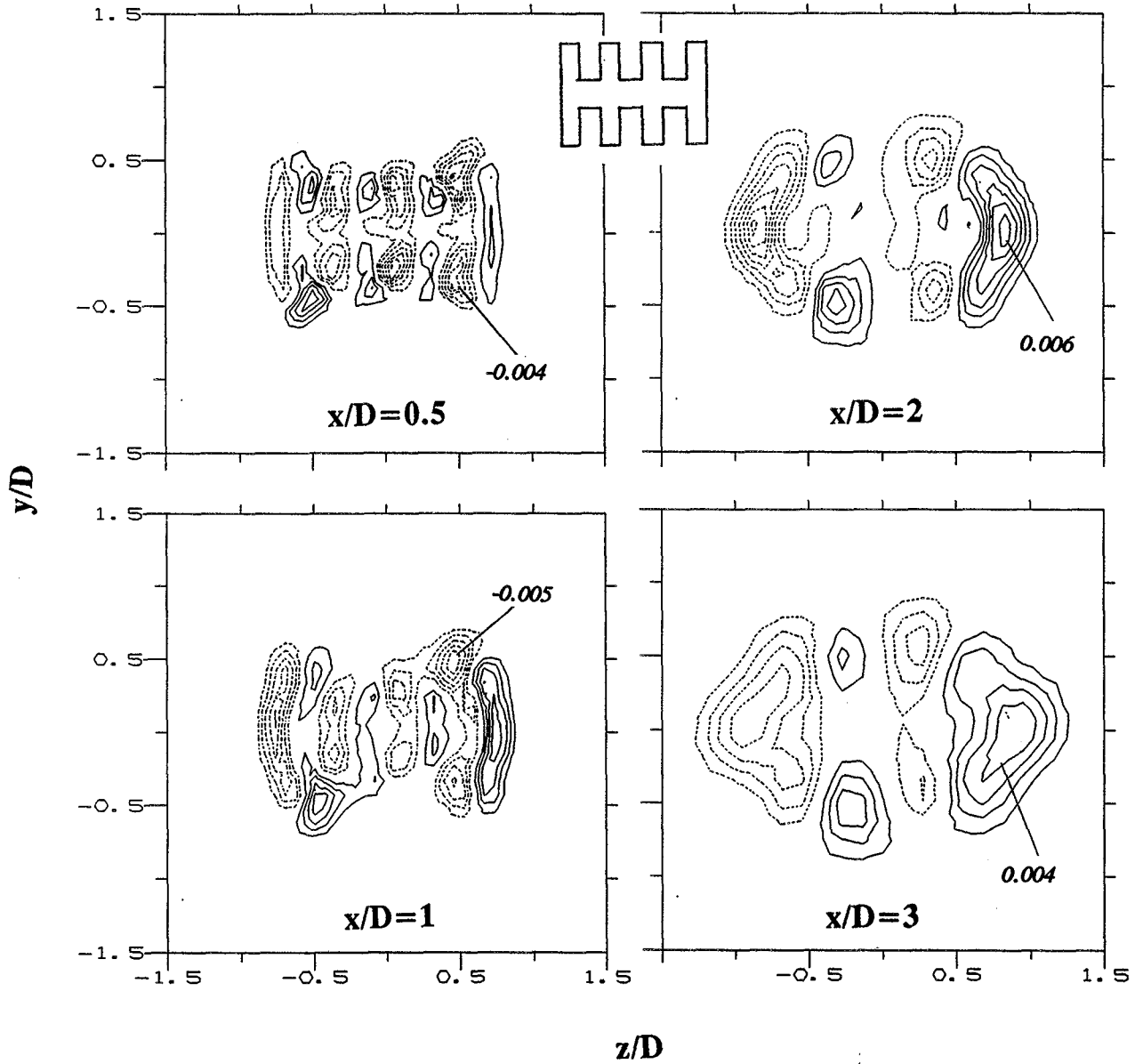


FIG. A17(c)

u'/U_j -CONTOURS; $x/D = 2$, $M_j = 0.31$

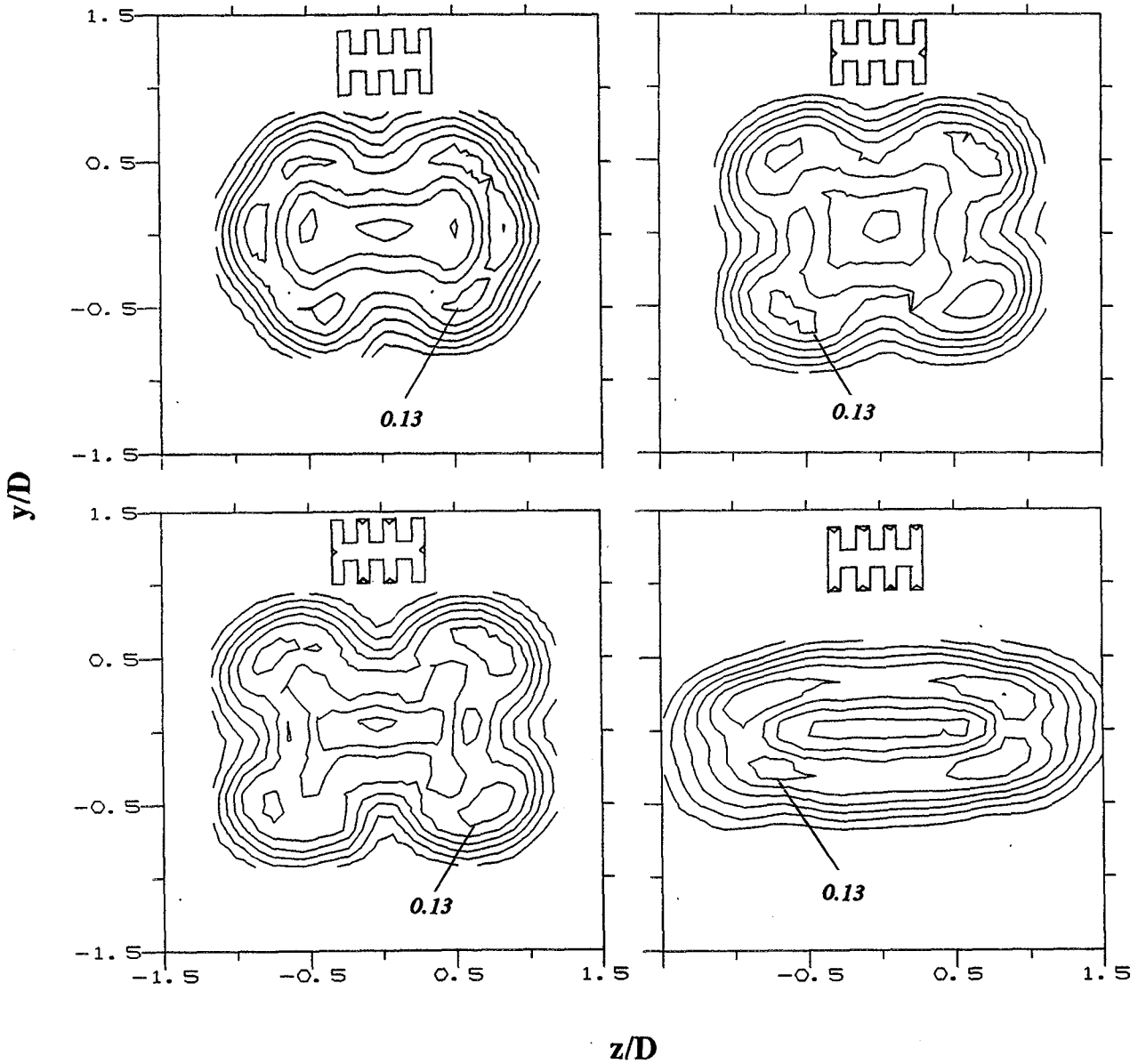


FIG. A18(a)

\overline{uv}/U_j^2 -CONTOURS; $x/D = 2$, $M_j = 0.31$

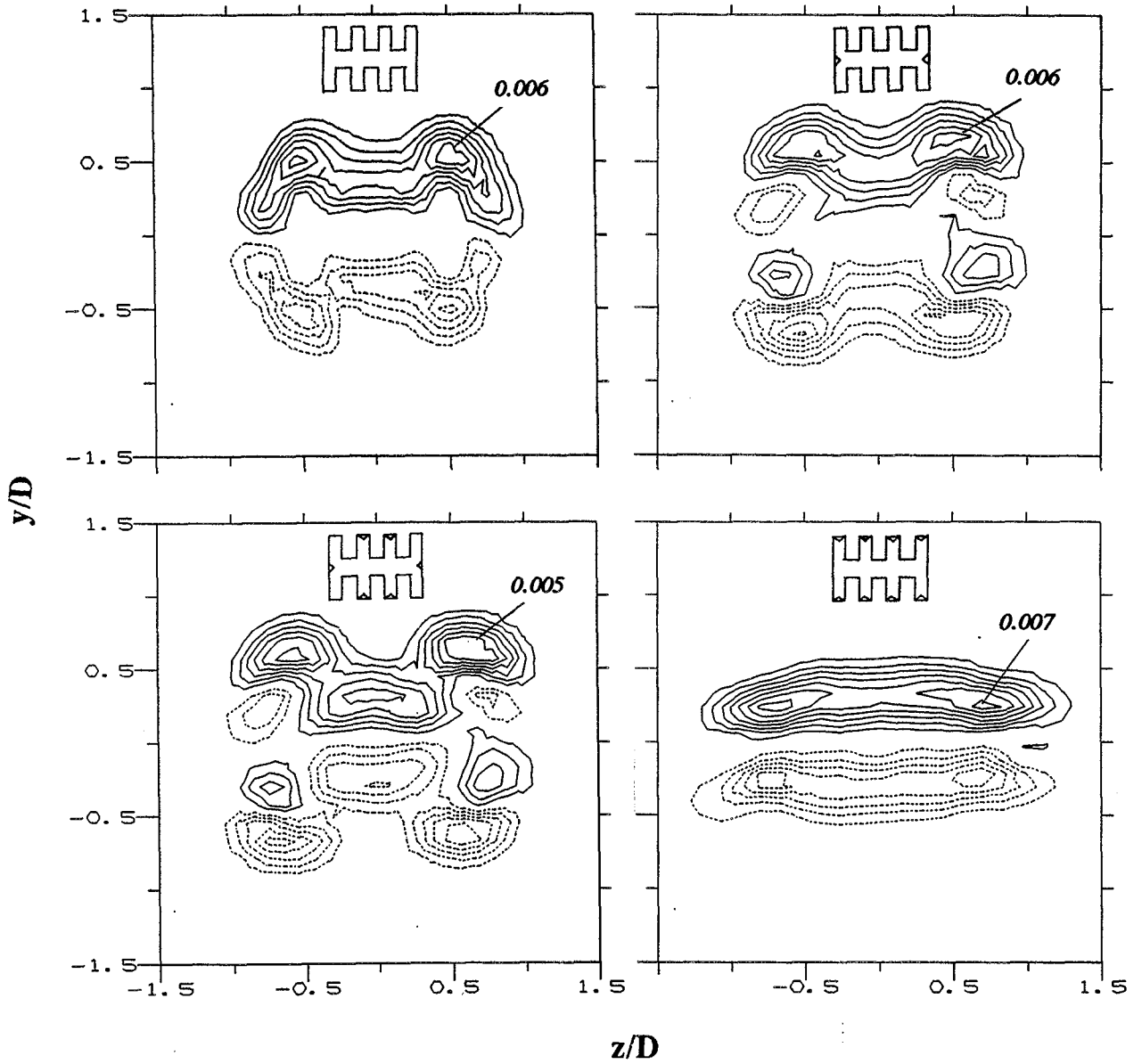


FIG. A18(b)

\overline{uw}/U_j^2 -CONTOURS; $x/D = 2$, $M_j = 0.31$

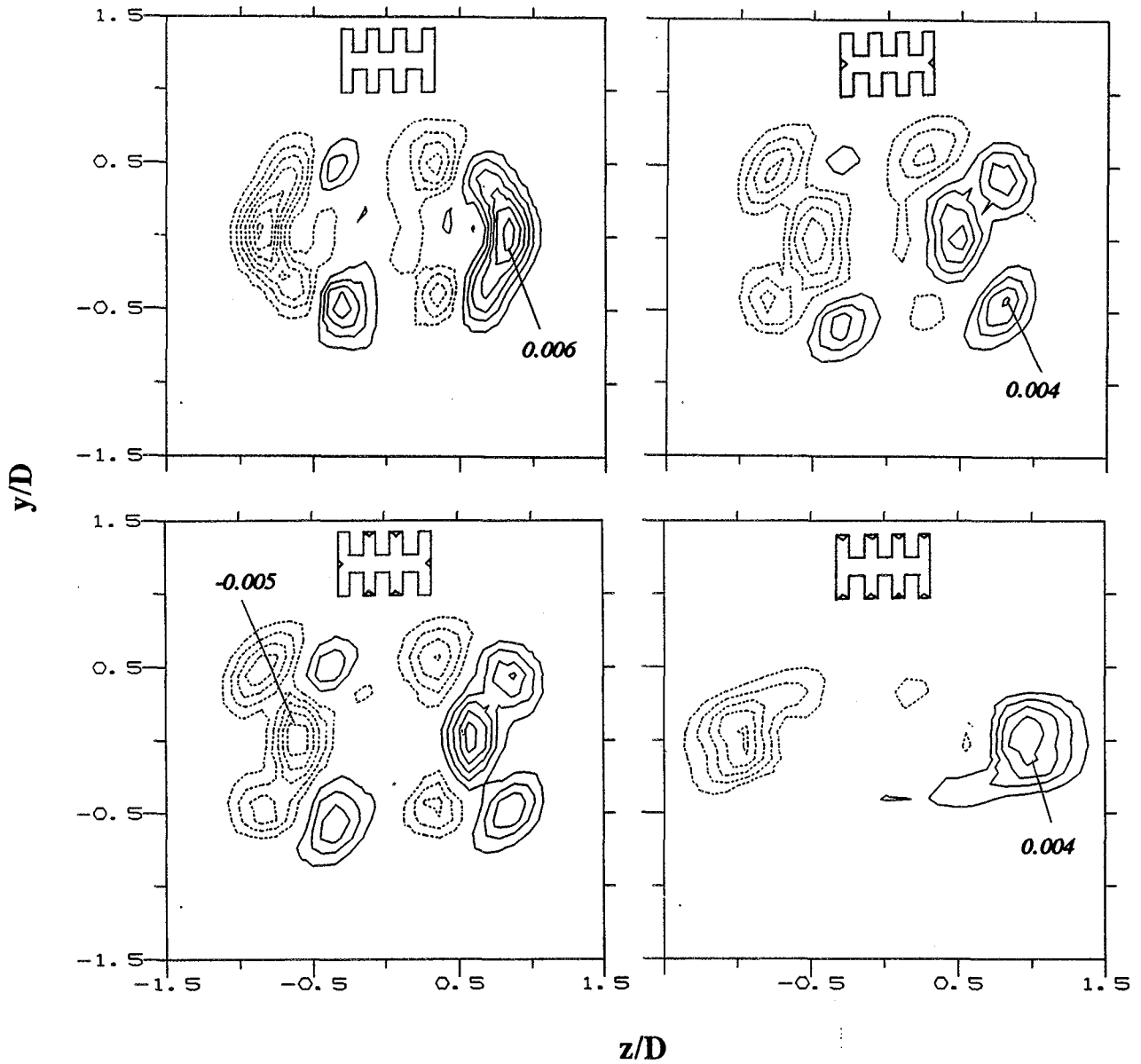
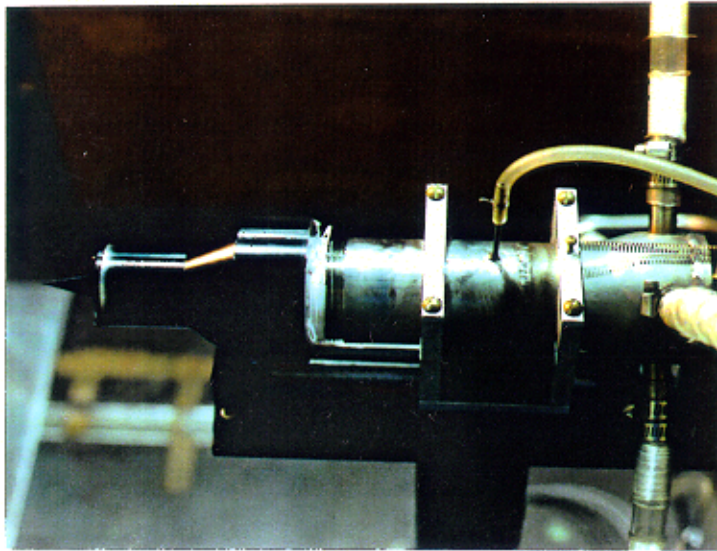


FIG. A18(c)

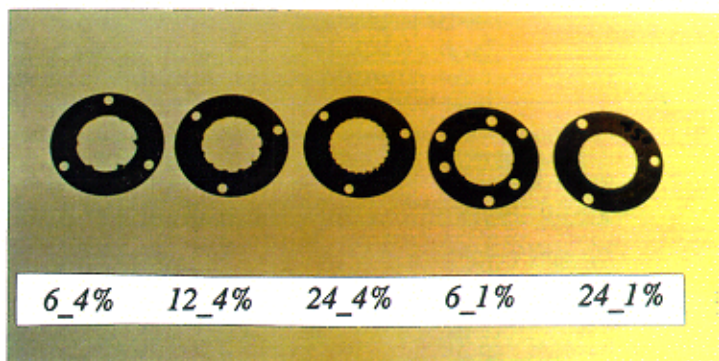
'ACE NOZZLE' MODEL



EXPERIMENTAL FACILITY



NOZZLE WITH POINTED PLUG



TAB DISCS

FIG. B1

SCHEMATIC OF NOZZLE ASSEMBLY

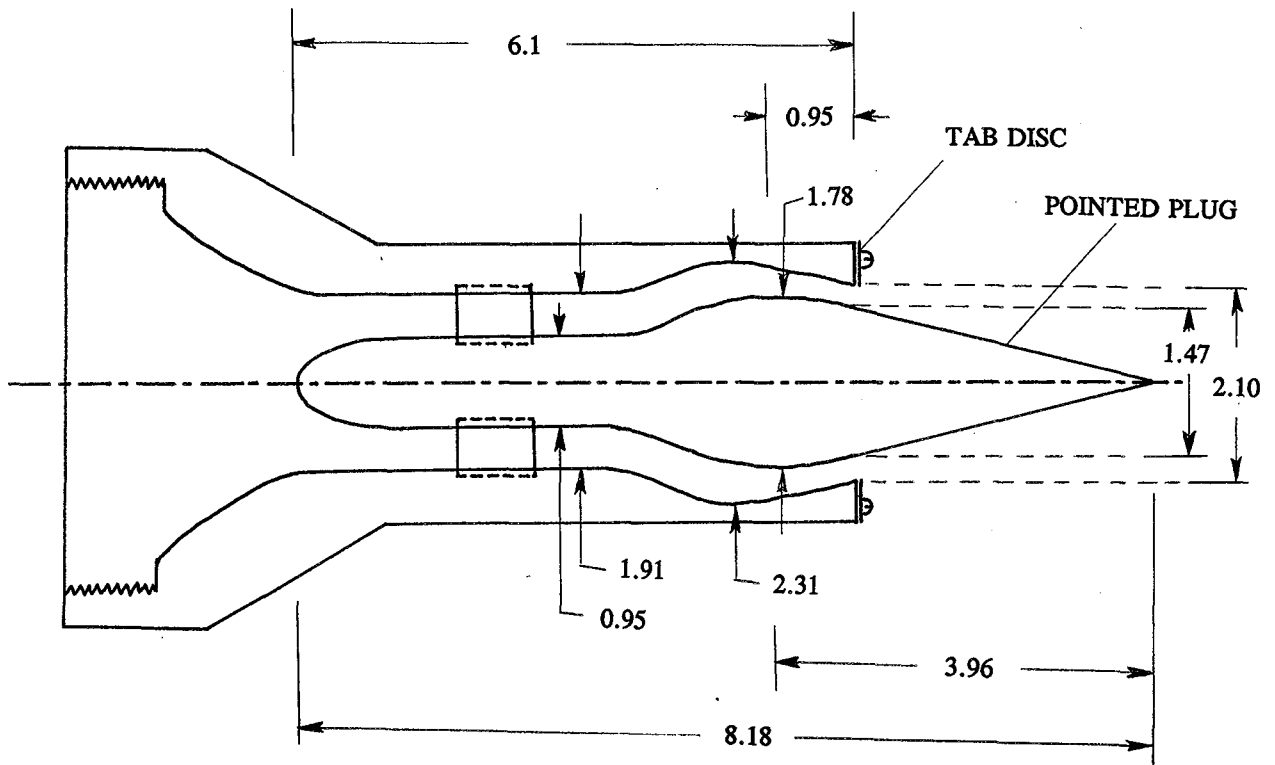


FIG. B2(a)

SCHEMATIC OF ROUNDED PLUGS

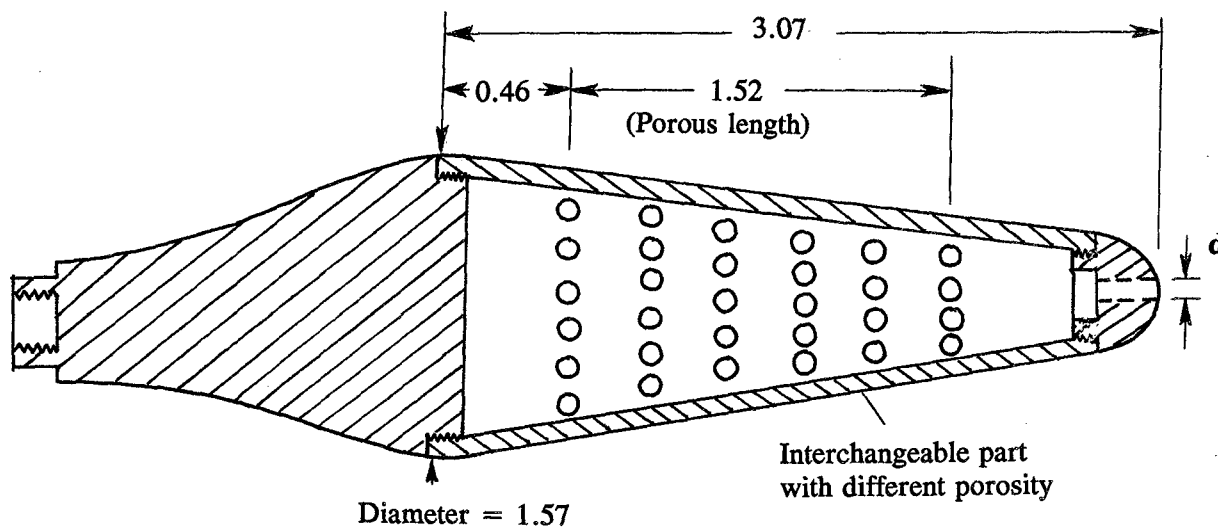
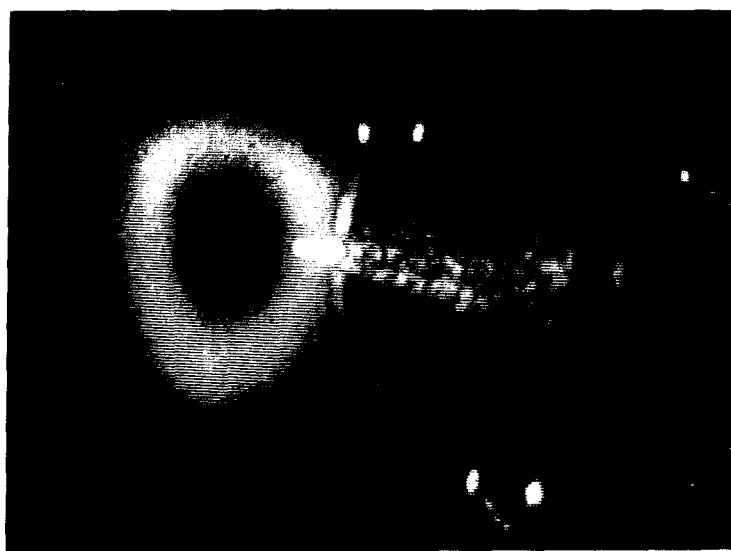


FIG. B2(b)

**LASER SHEET
FLOW VISUALIZATION
POINTED PLUG
 $M_j = 1.63$**



NO TAB



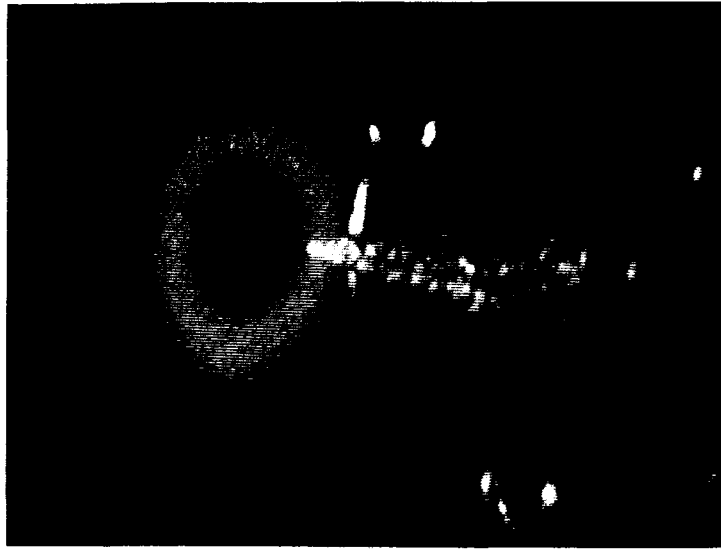
24_1%



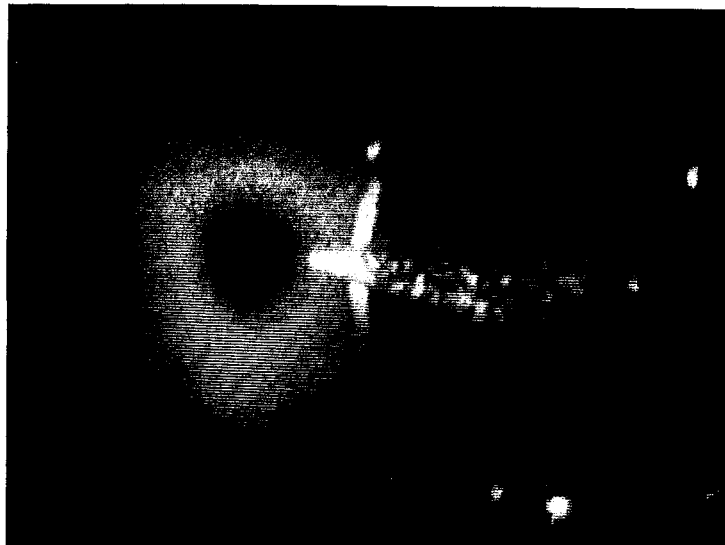
6_1%

FIG. B3(a)

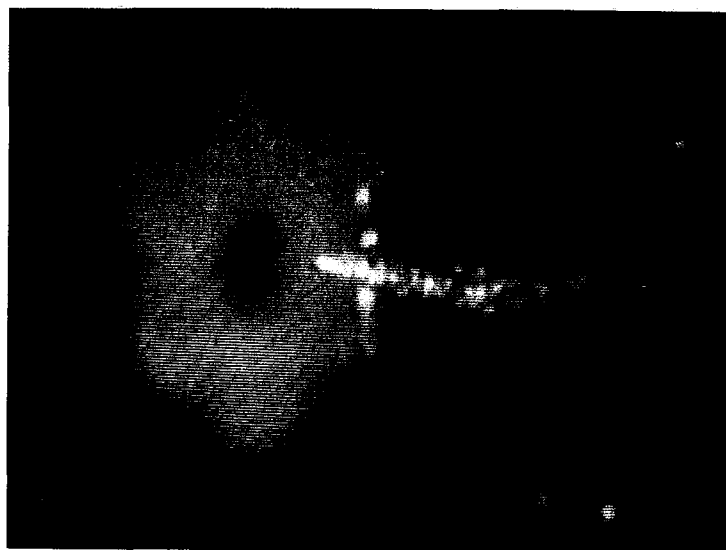
**LASER SHEET
FLOW VISUALIZATION
POINTED PLUG
 $M_j = 1.63$**



24_4%



12_4%



6_4%

FIG. B3(b)

LASER SHEET FLOW VISUALIZATION
FOR INDICATED PLUG & TAB CONFIGS., $M_j = 1.63$

SOLID PLUG

5.5%H PLUG

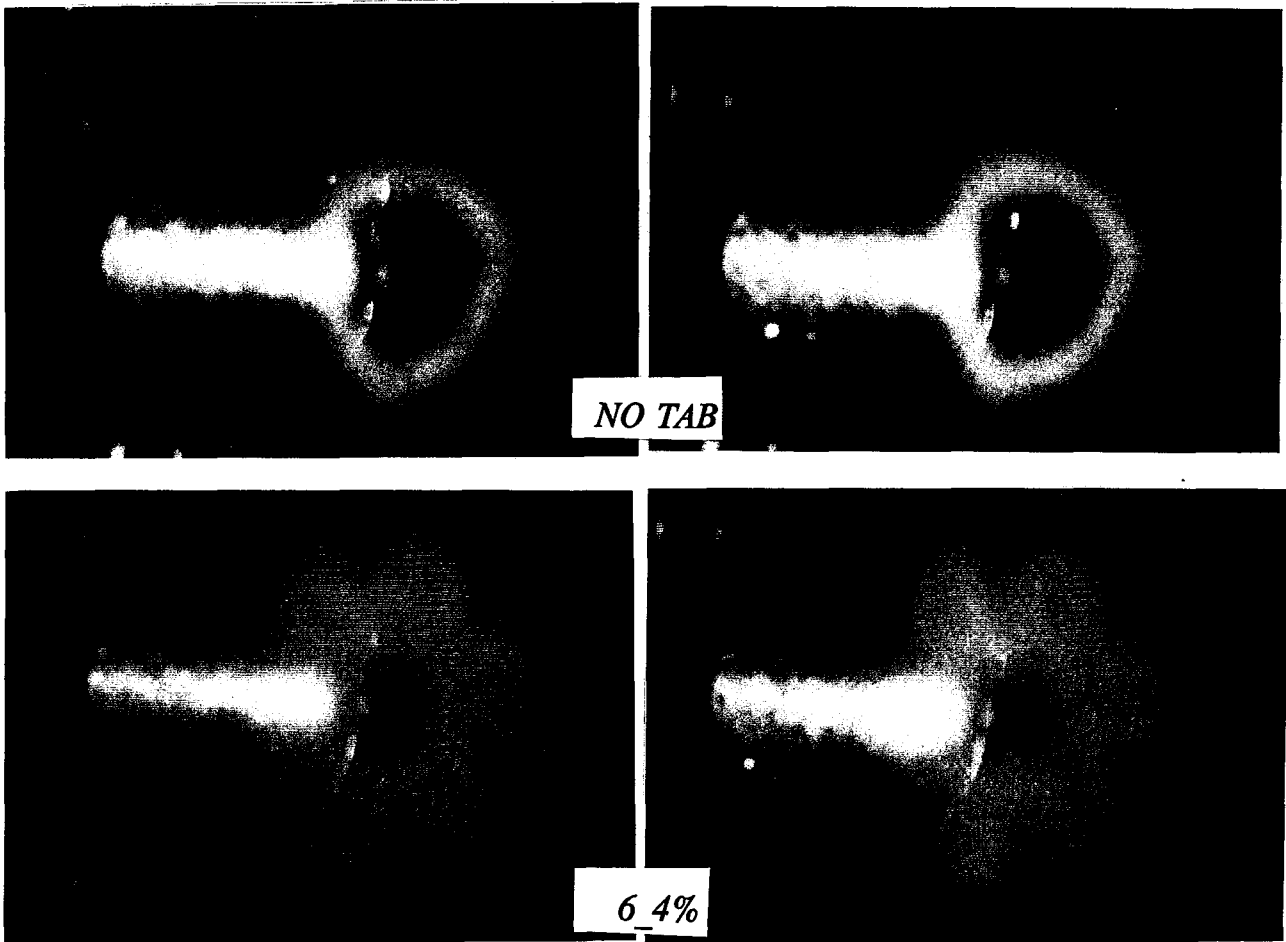


FIG. B4

**SCHLIEREN PHOTOGRAPHS
FOR INDICATED PLUG & TAB CONFIGS., $M_j = 1.63$**

SOLID PLUG

5.5%H PLUG

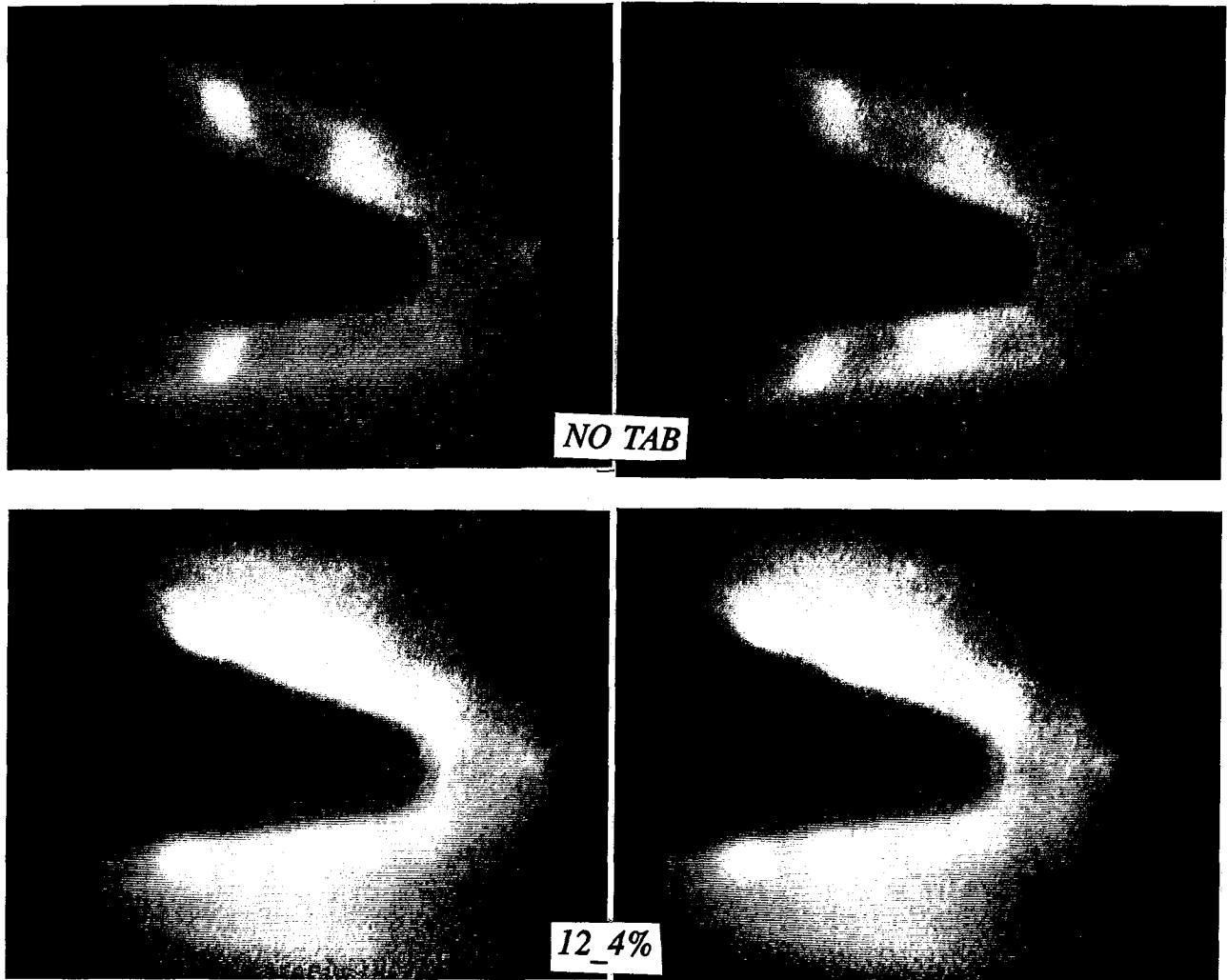


FIG. B5(a)

**SCHLIEREN PHOTOGRAPHS
FOR SOLID PLUG, $M_j = 1.63$**

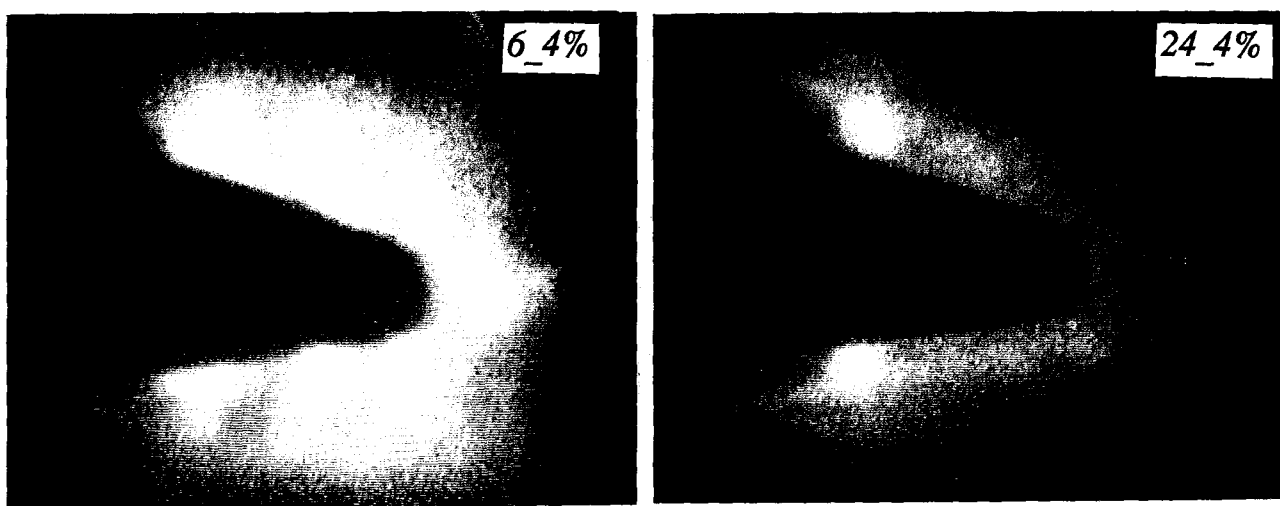


FIG. B5(b)

THRUST VS. NPR
COMPARISON OF FIVE PLUG CASES

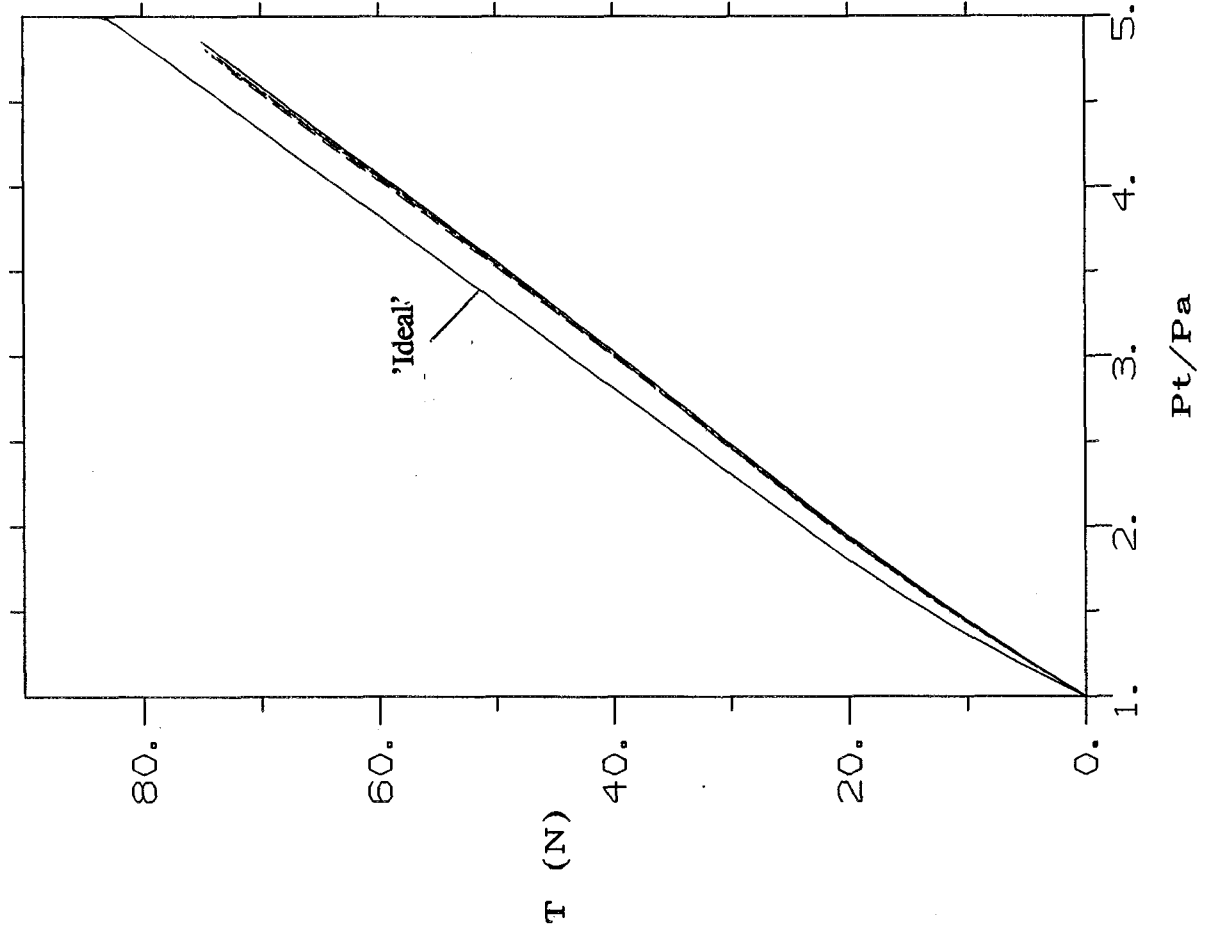


FIG. B6

i	tab	descrip	%loss_4.47
86	0	ace_notab_new	6.1
90	0	ace_8.2%H_05	6.3
91	0	ace_5.5%H_05	6.2
92	0	ace_3.6%H_05	5.7
93	0	ace_10%S_05	6.9

AT Pt/Pa=4.47:

i	%blk	cd0	cf1	cf2
86	10.2	0.730	0.991	0.968
90	10.6	0.730	0.991	0.968
91	10.7	0.730	0.993	0.970
92	10.5	0.730	0.997	0.974
93	10.1	0.730	0.982	0.959

th cal # 70

mdot cal # 71

Date 27-SEP-1994

Data: 27-SEP-1994

09:04:12

[zaman.osc]zth--p2

THRUST VS. NPR
5.5%H PLUG PLUS DIFFERENT END HOLES

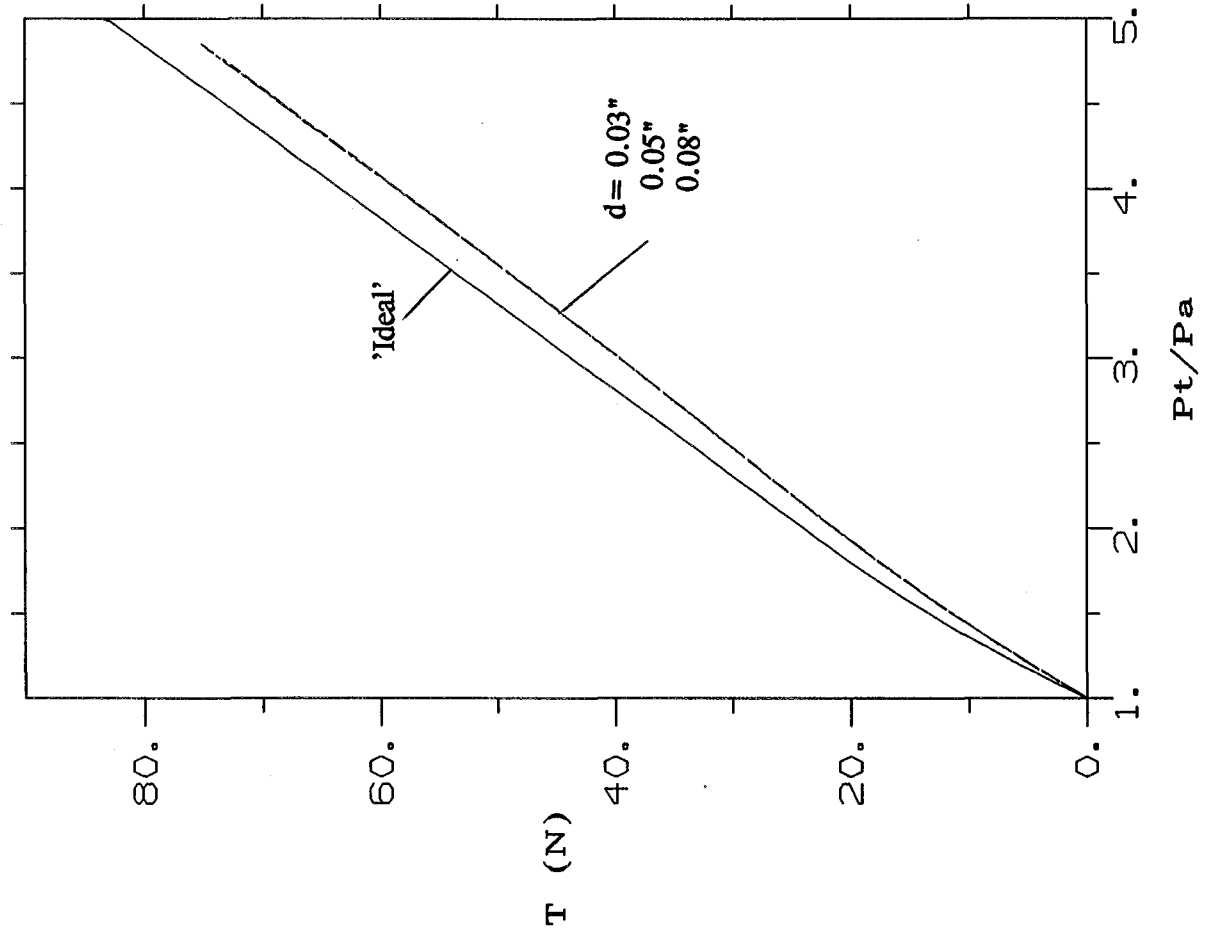


FIG. B7

i	tab	descrip	%loss_4.47
97	0	ace_5.5%H_03	6.8
98	0	ace_5.5%H_05	rB.7
99	0	ace_5.5%H_08	6.6

AT Pt/Pa=4.47:

i	%blkg	cd0	cf1	cf2
97	10.3	0.730	0.984	0.961
98	10.5	0.730	0.986	0.963
99	10.3	0.730	0.986	0.964

th cal # 70
 mndot cal # 71
 Date 27-SEP-1994
 Data: 27-SEP-1994
 11:23:29

[zaman.osc]zth_p2

THRUST VS. NPR
FOUR TAB CASES WITH SOLID PLUG

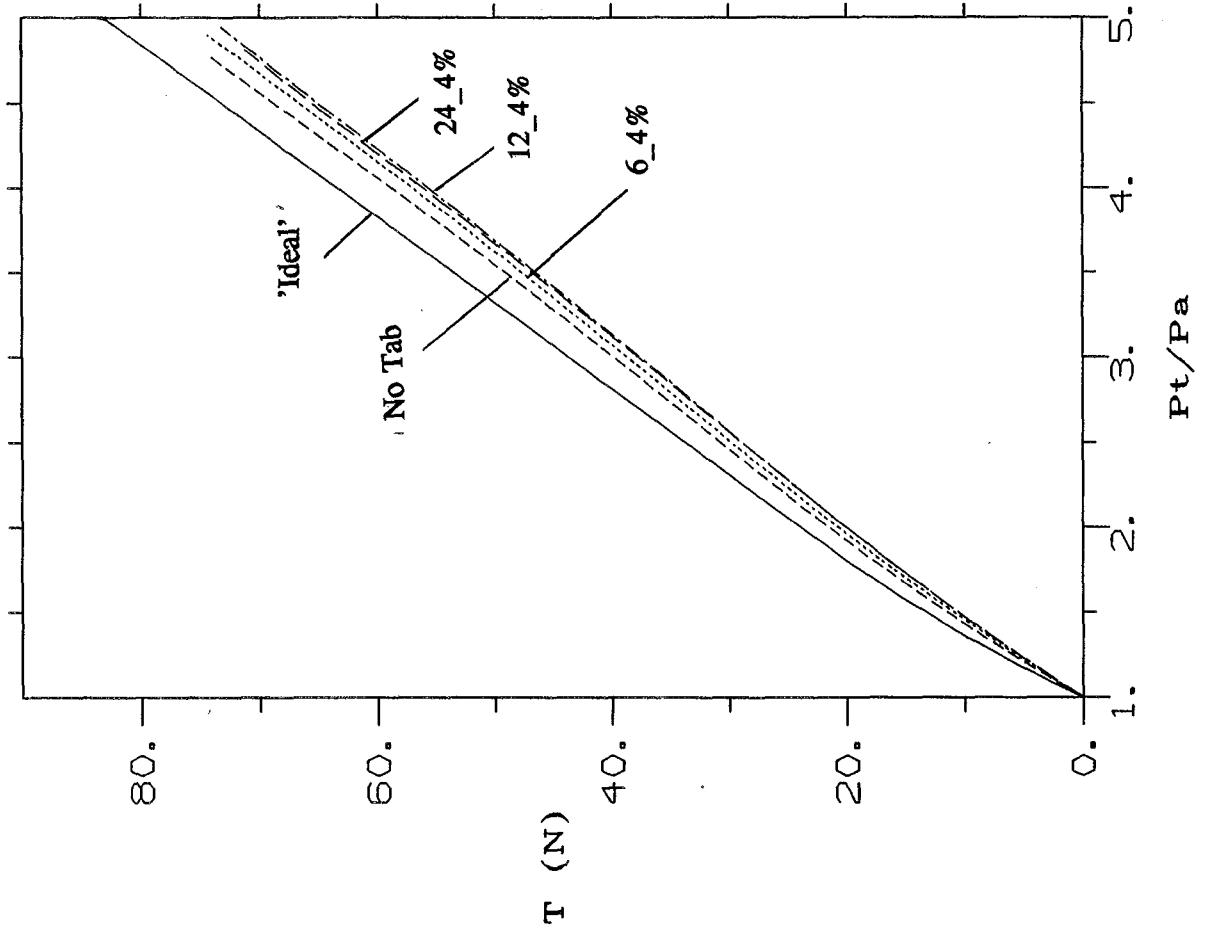


FIG. B8

i	tab	descrip.	%loss_4.47
86	0	ace_notab_new	6.1
87	6	ace_6_4%_new	9.1
88	12	ace_12_4%_new	11.3
89	24	ace_24_4%_new	10.6

AT Pt/Pa=4.47:

i	%blkg	cd0	cf1	cf2
86	10.2	0.730	0.991	0.968
87	12.7	0.730	0.973	0.950
88	16.5	0.731	0.971	0.949
89	14.8	0.730	0.969	0.946

th cal # 70

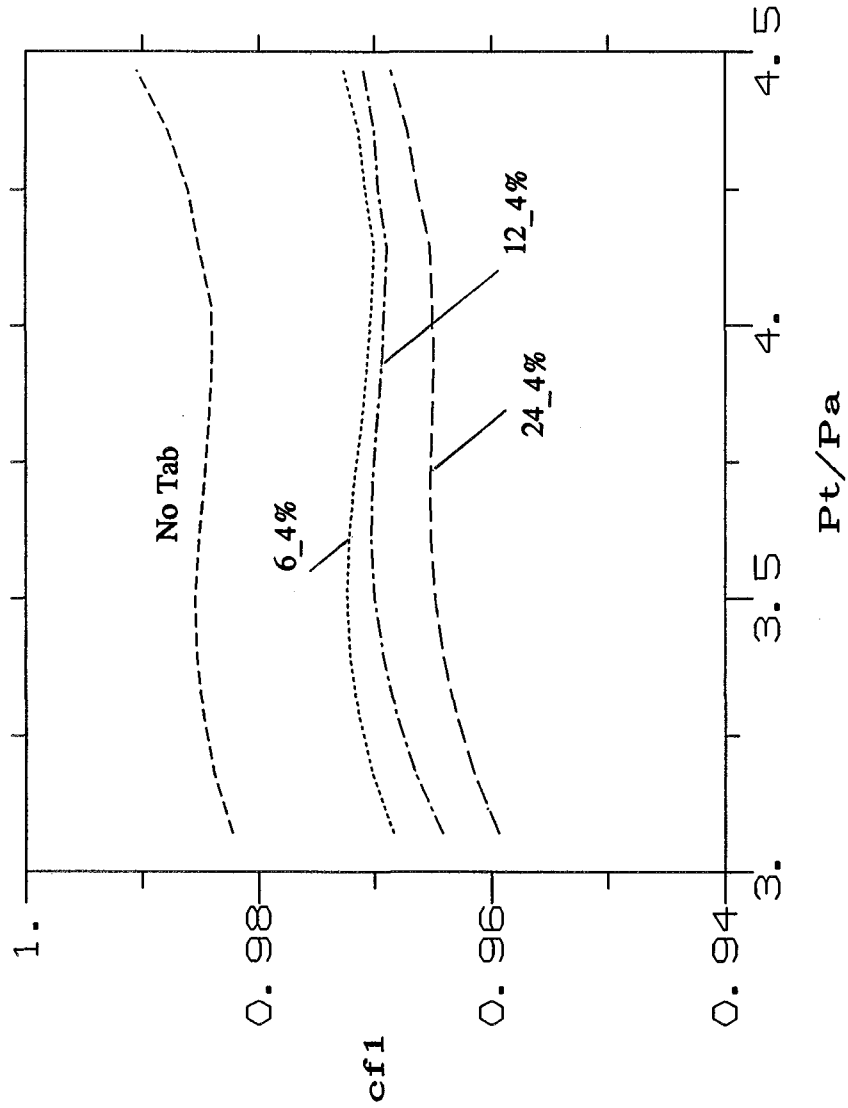
mdot cal # 71

Date 27-SEP-1994

Data: 27-SEP-1994
08:06:56

[zaman.osc]zth-p2

THRUST COEFFICIENT VS. NPR
 FOUR TAB CASES WITH SOLID PLUG

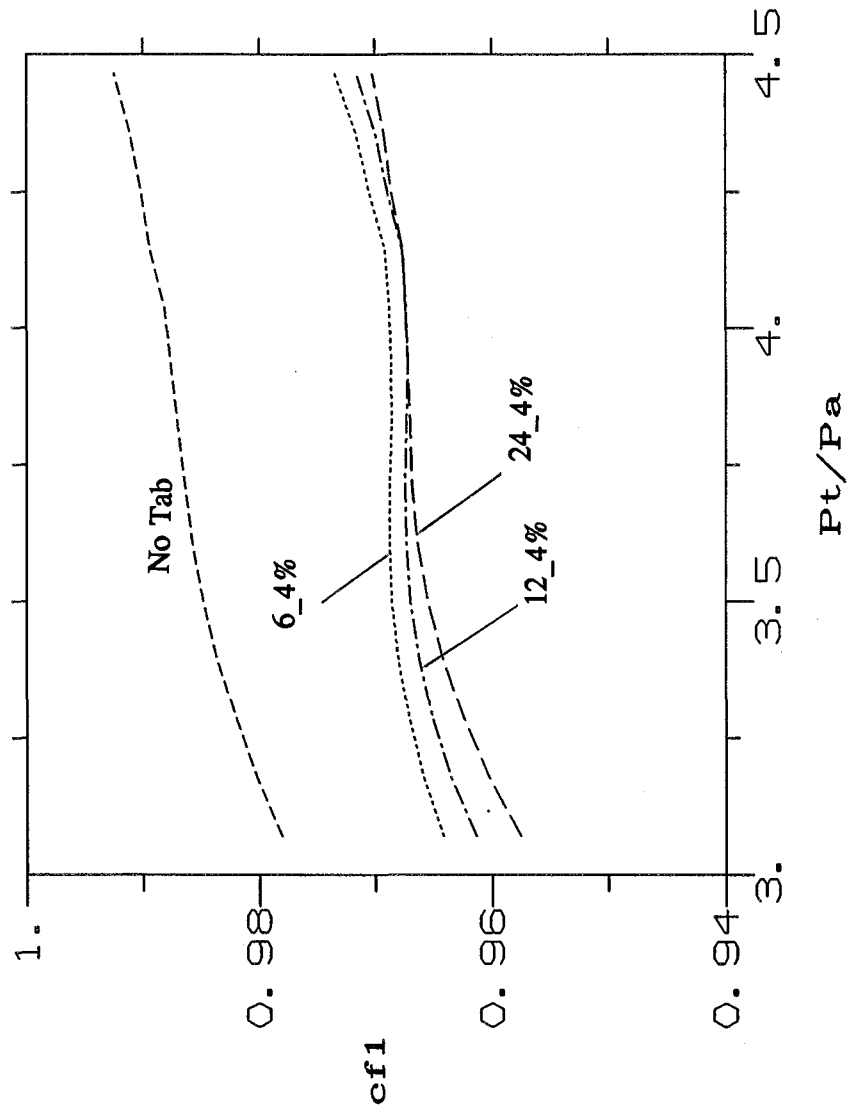


i	tab	descrip
86	0	ace_notab_new
87	6	ace_6_4%_new
88	12	ace_12_4%_new
89	24	ace_24_4%_new

th cal # 70
 mdot cal # 71
 Plot on 27-SEP-1994
 Data: 27-SEP-1994
 08:06:56
 [zaman.osc]zth-p3

FIG. B9

THRUST COEFFICIENT VS. NPR
 FOUR TAB CASES WITH 5.5%H PLUG



i	tab	descrip
91	0	ace-5.5%H-05
94	6	ace-5.5%H-05T
95	12	ace-5.5%H-05T
96	24	ace-5.5%H-05T

th cal # 70
 mdot cal # 71
 Plot on 27-SEP-1994
 Data: 27-SEP-1994
 10:08:50
 [zaman.osc]zth-p3

FIG. B10

FAR FIELD NOISE, NPR \approx 4.5
 EFFECT OF FOUR POROUS PLUGS
 (DASHED LINE FOR SOLID PLUG)

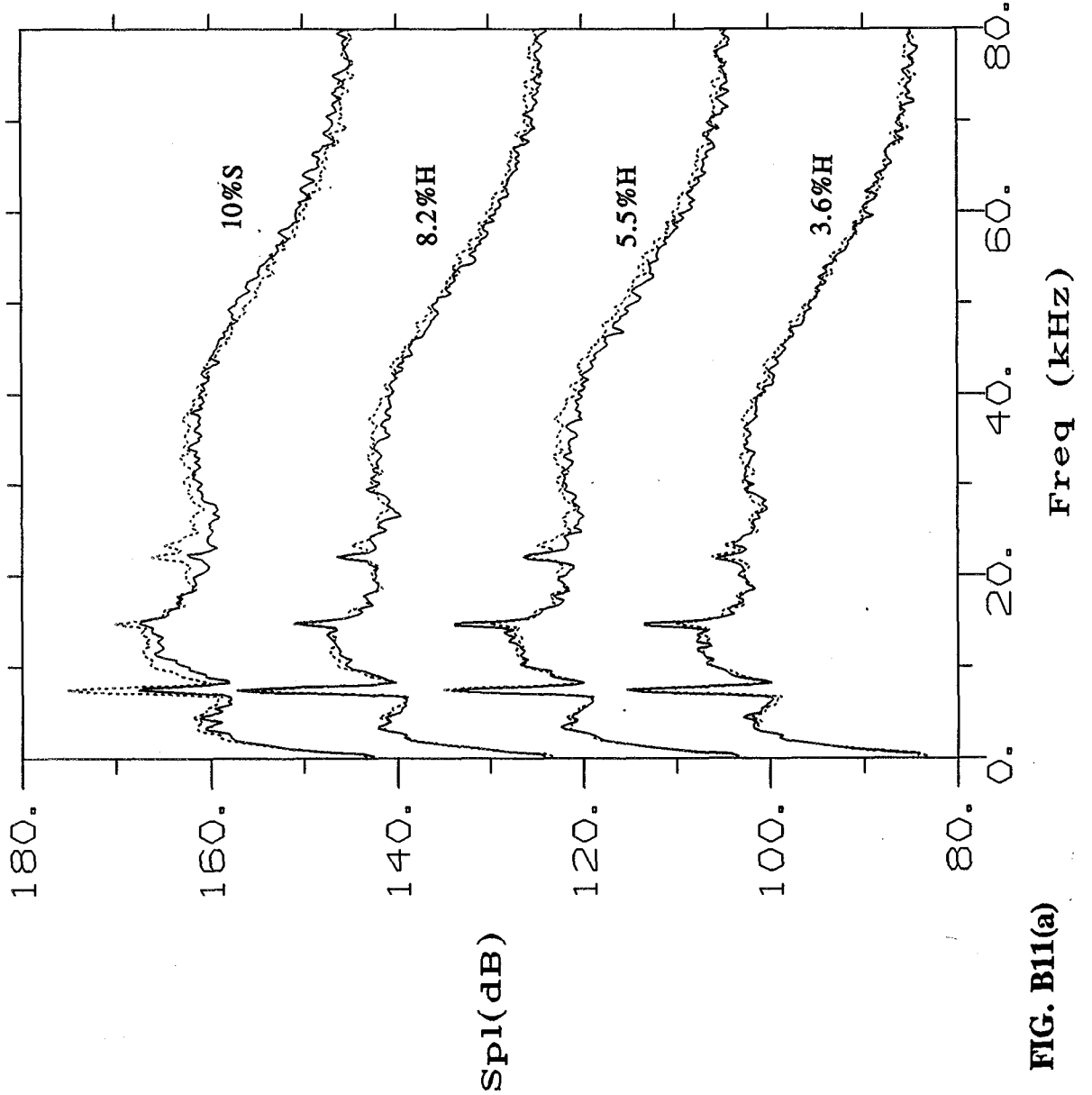


FIG. B11(a)

Nozzle 8

Date 27-SEP-1994

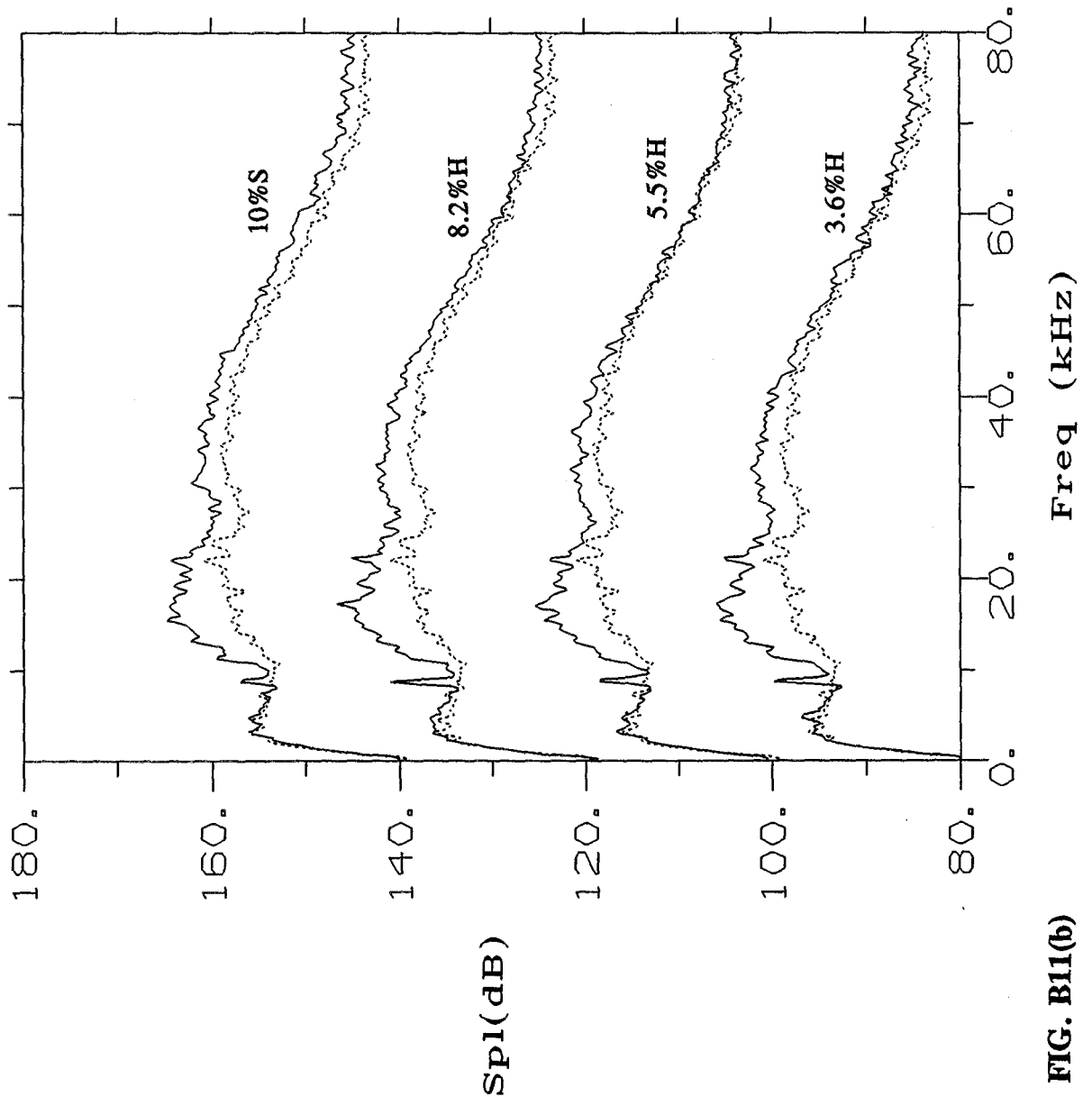
Time 13:23:03

rec	Mj	scr-f	scr-a	oaspl:
291	1.619	7.50	116.4	123.8
290	1.619	7.50	116.1	123.3
288	1.621	7.50	114.0	123.2
290	1.619	7.50	116.1	123.3
292	1.618	7.50	117.2	123.9
290	1.619	7.50	116.1	123.3
293	1.620	7.50	107.6	121.6
290	1.619	7.50	116.1	123.3

plot on 28-SEP-1994

[zaman.ssj] read_spect

FAR FIELD NOISE, NPR ~ 3.5
EFFECT OF FOUR POROUS PLUGS
(DASHED LINE FOR SOLID PLUG)



Nozzle 8

Date 5-OCT-1994

Time 13:19:30

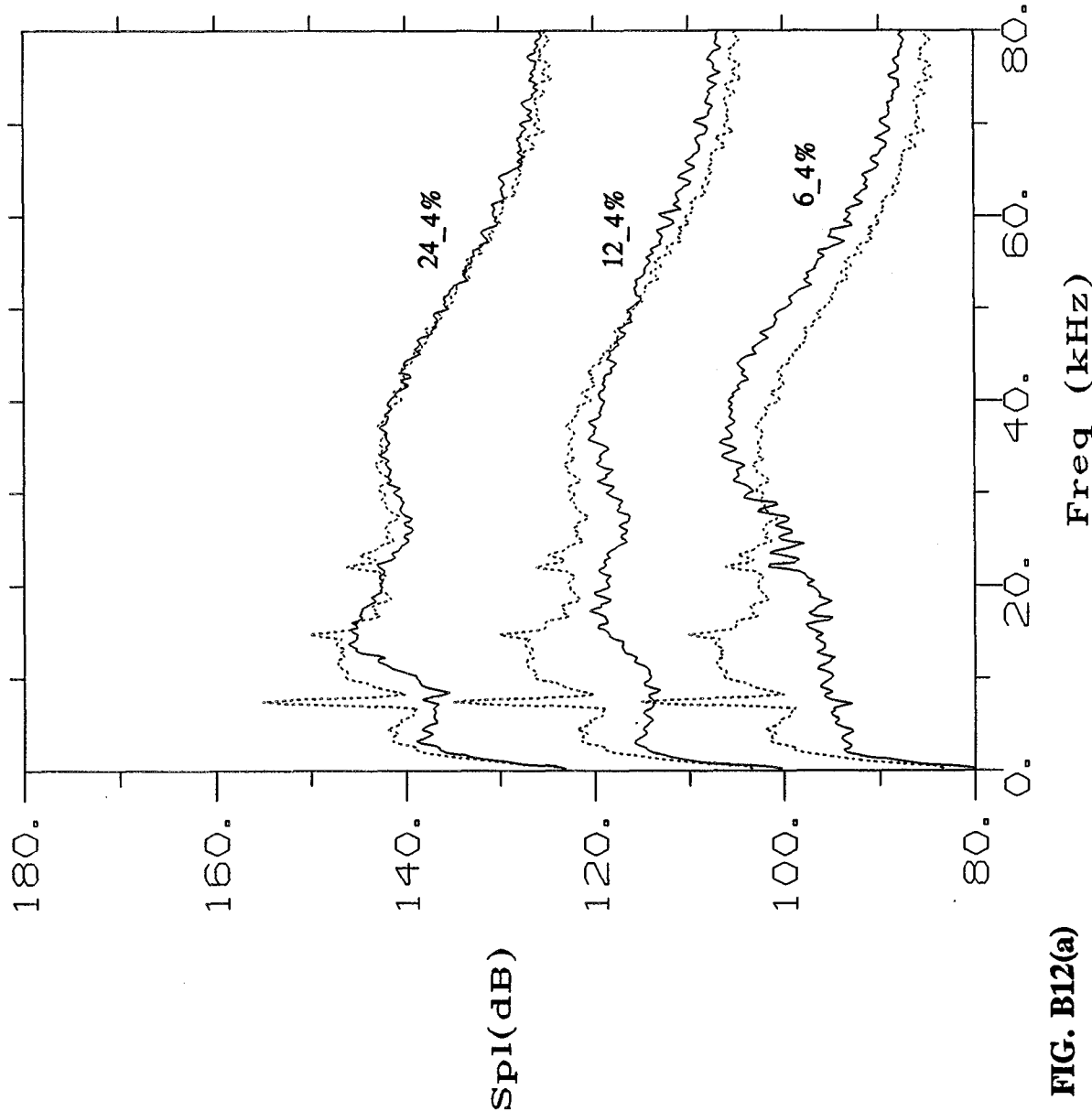
rec	Mj	scr_f	scr_a	oaspl:
307	1.451	17.25	106.0	120.4
306	1.448	22.00	100.9	116.4
308	1.444	17.00	105.3	119.6
306	1.448	22.00	100.9	116.4
309	1.456	17.25	106.7	120.6
308	1.448	22.00	100.9	116.4
310	1.446	15.50	104.8	119.9
306	1.448	22.00	100.9	116.4

plot on 5-OCT-1994

[zaman.ssj] read_spect

FIG. B11(b)

FAR FIELD NOISE, NPR \approx 4.5
 EFFECT OF THREE TAB CASES TOGETHER WITH 5.5% H PLUG
 (DASHED LINE FOR SOLID PLUG, NO TAB CASE)



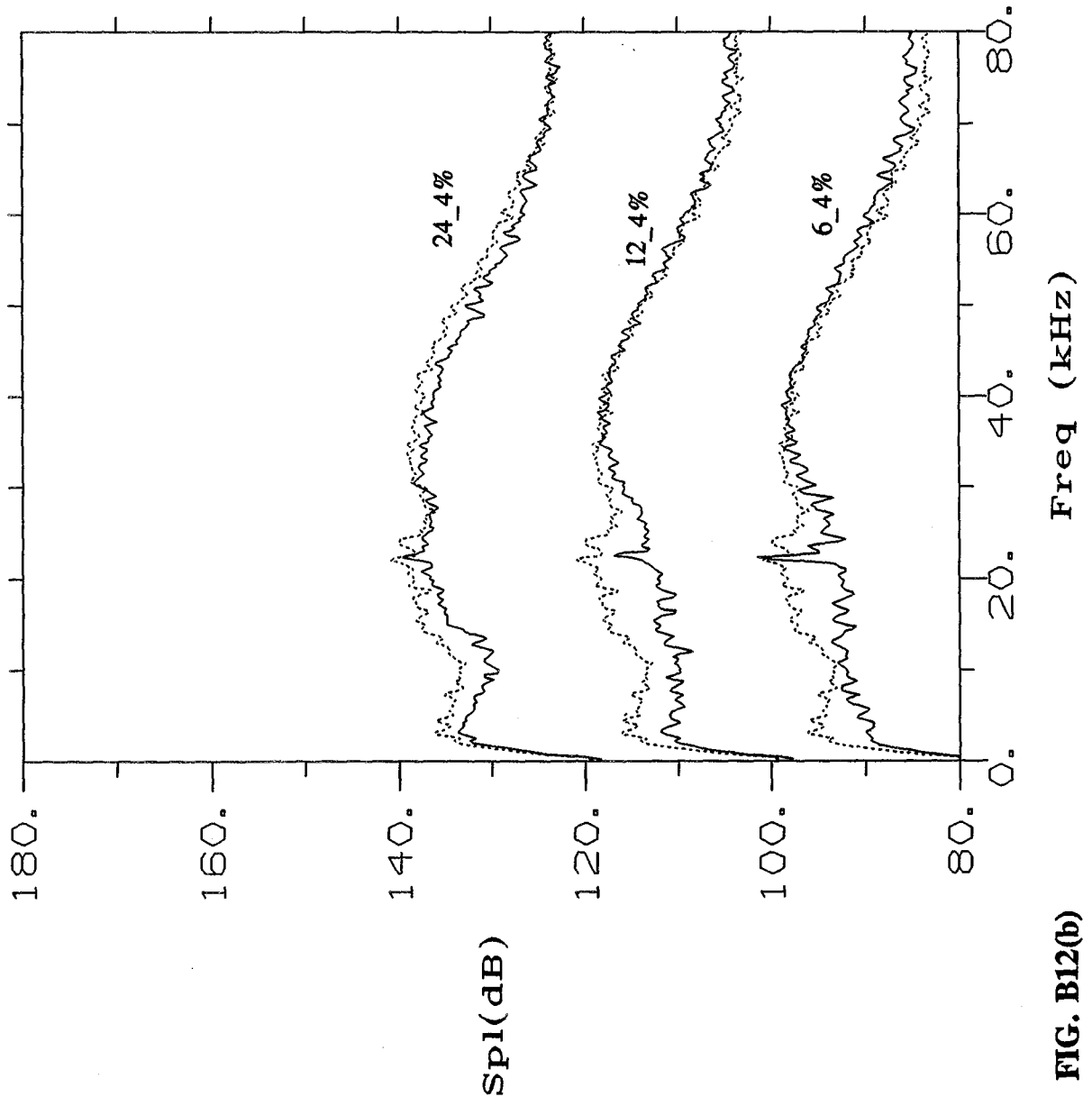
Nozzle 8
 Date 27-SEP-1994
 Time 13:23:03

rec	Mj	scr_f	scr_a	oaspl:
301	1.626	36.50	106.8	121.7
290	1.619	7.50	115.1	123.3
302	1.621	37.75	100.6	117.5
290	1.619	7.50	115.1	123.3
305	1.625	13.75	106.1	121.1
290	1.618	7.50	115.1	123.3

plot on 28-SEP-1994
 [zaman.ssj] read_spect

FIG. B12(a)

FAR FIELD NOISE, NPR ≈ 3.5
 EFFECT OF THREE TAB CASES TOGETHER WITH 5.5% H PLUG
 (DASHED LINE FOR SOLID PLUG, NO TAB CASE)



Nozzle 8

Date 5-OCT-1994

Time 13:19:30

rec	MJ	scr_f	scr_a	oaspl:
314	1.442	22.25	101.5	114.6
306	1.448	22.00	100.9	116.4
316	1.447	38.25	98.7	114.0
306	1.448	22.00	100.9	116.4
318	1.446	22.25	99.6	114.2
306	1.448	22.00	100.9	116.4

plot on 5-OCT-1994

[zaman.ssj] read_spect

FAR FIELD NOISE, NPR ≈ 4.5
 COMPARISON OF SOLID PLUG AND 5.5% H PLUG DATA
 FOR FOUR TAB CASES

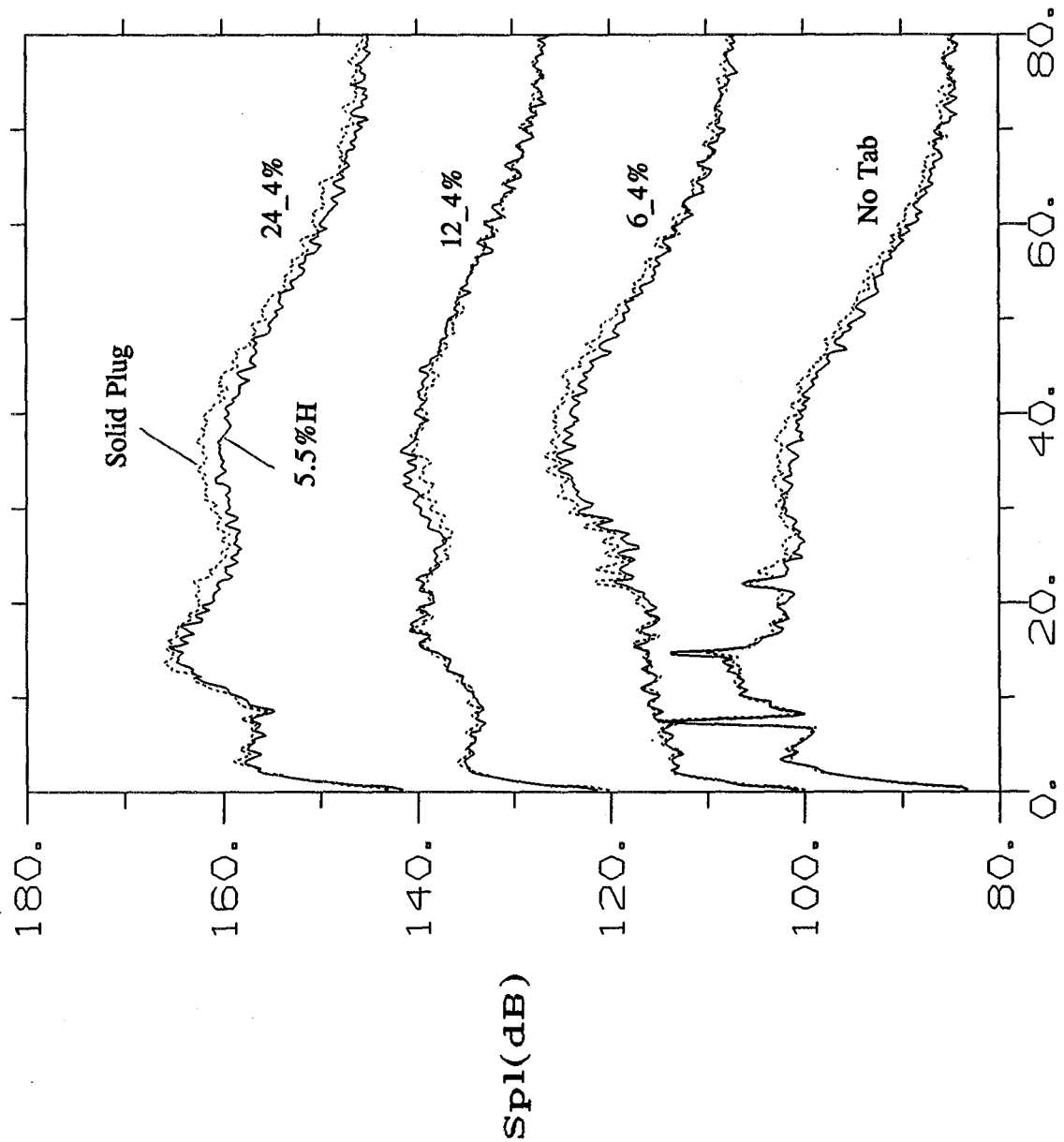


FIG. B13(a)

Nozzle 8

Date 27-SEP-1994

Time 14:12:59

rec	Mj	scr-f	scr-a	oaspl:
288	1.621	7.50	114.0	129.2
290	1.619	7.50	116.1	123.3
300	1.622	35.50	105.4	120.6
301	1.626	35.50	106.8	121.7
303	1.623	36.00	101.8	118.3
302	1.621	37.75	100.6	117.5
304	1.625	15.25	105.4	119.7
305	1.625	13.75	106.1	121.1

plot on 28-SEP-1994

[zaman.msj] read_spect

FAR FIELD NOISE, NPR ~ 3.5
 COMPARISON OF SOLID PLUG AND 5.5% H PLUG DATA
 FOR FOUR TAB CASES

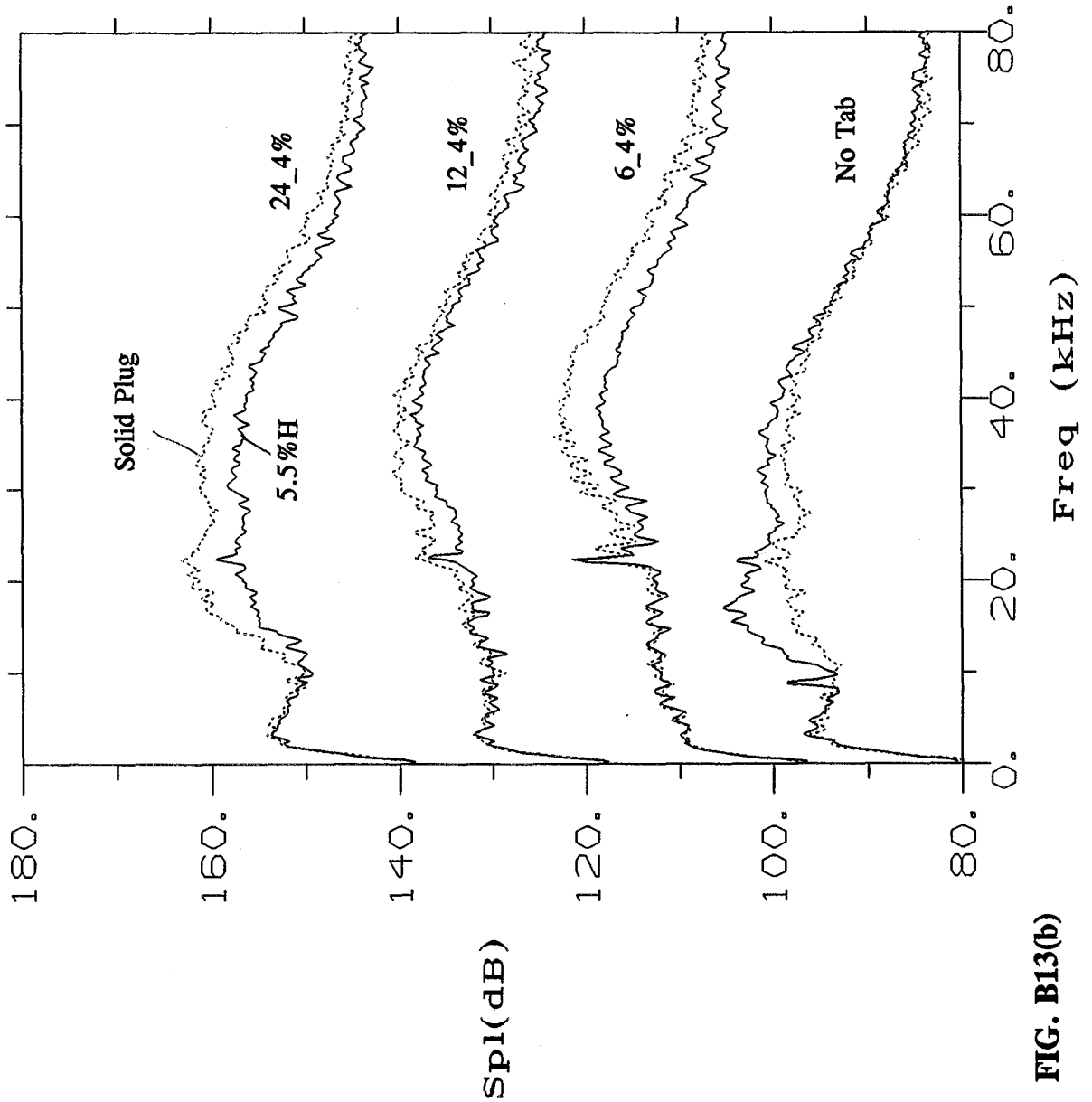


FIG. B13(b)

Nozzle 8

Date 5-OCT-1994

Time 14:09:40

rec	Mj	scr_f	scr_a	oaspl:
308	1.444	17.00	105.3	119.6
306	1.448	22.00	100.9	116.4
314	1.442	22.25	101.5	114.6
313	1.444	35.75	103.4	118.3
316	1.447	38.25	98.7	114.0
315	1.455	32.00	100.6	116.6
318	1.446	22.25	99.6	114.2
317	1.445	22.25	103.3	118.6

plot on 5-OCT-1994

[zaman.ssj] read_spect

FAR FIELD NOISE
COMPARISON OF 5.5% H PLUG AND SOLID PLUG DATA (NO TAB)
AT FOUR MACH NUMBERS

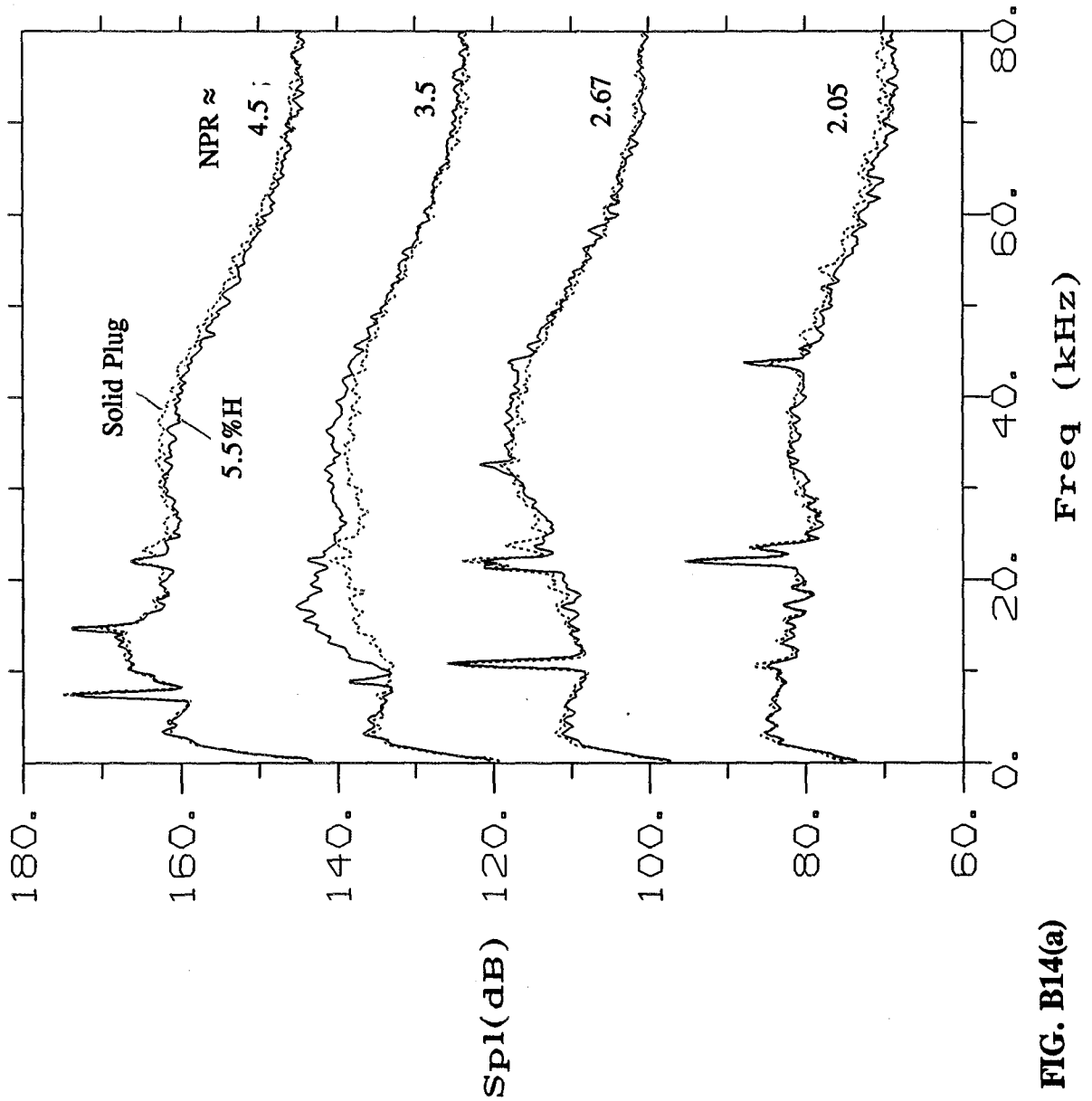
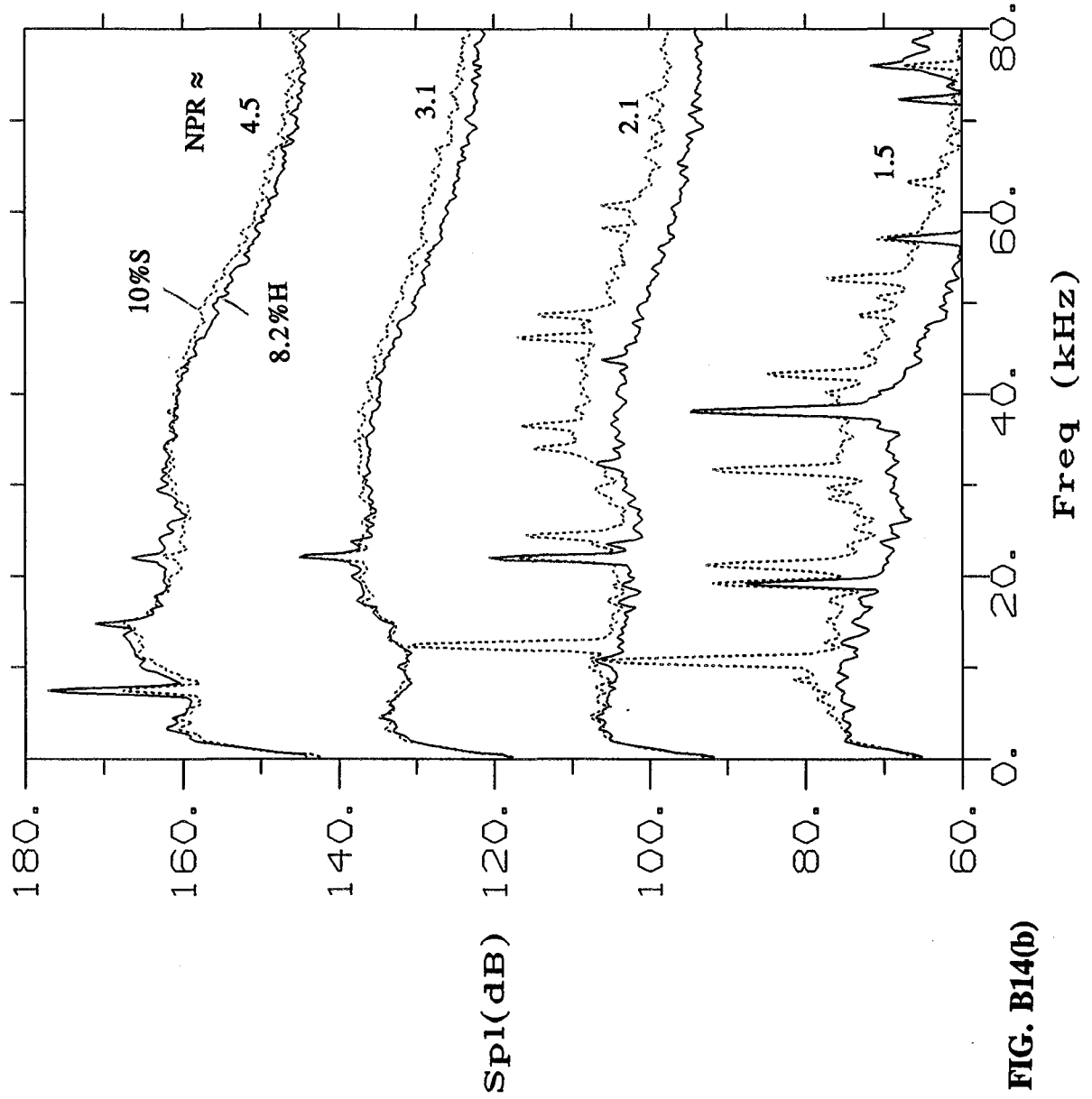


FIG. B14(a)

**FAR FIELD NOISE
COMPARISON OF 8.2%H PLUG AND 10%S PLUG DATA (NO TAB)
AT FOUR MACH NUMBERS**



Nozzle 8

Date 27-SEP-1994

Time 13:34:09

rec	Mj	scr_f	scr_a	ospl:
297	0.708	38.00	94.7	98.3
296	0.706	10.75	106.3	104.8
298	1.068	22.00	100.6	100.9
295	1.063	12.25	111.2	111.9
299	1.366	22.00	105.0	114.3
294	1.366	22.00	104.5	114.6
292	1.618	7.50	117.2	123.9
293	1.620	7.50	107.6	121.6

plot on 28-SEP-1994

[zaman.ssf] read_spect

FIG. B14(b)

FAR FIELD NOISE
EFFECT OF 12.4% TAB TOGETHER WITH SOLID PLUG
AT FOUR MACH NUMBERS

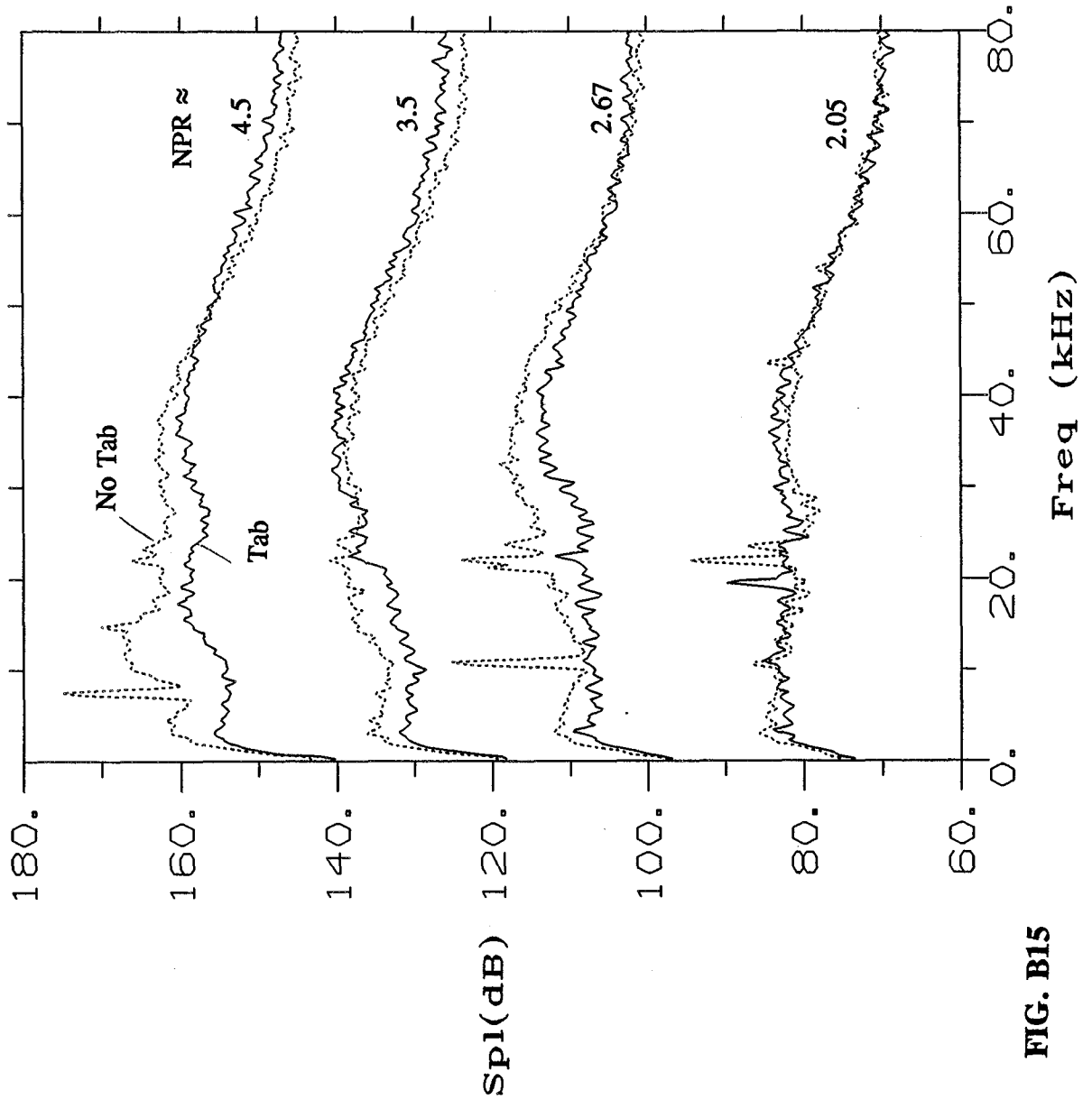


FIG. B15

Nozzle 8

Date 27-SEP-1994

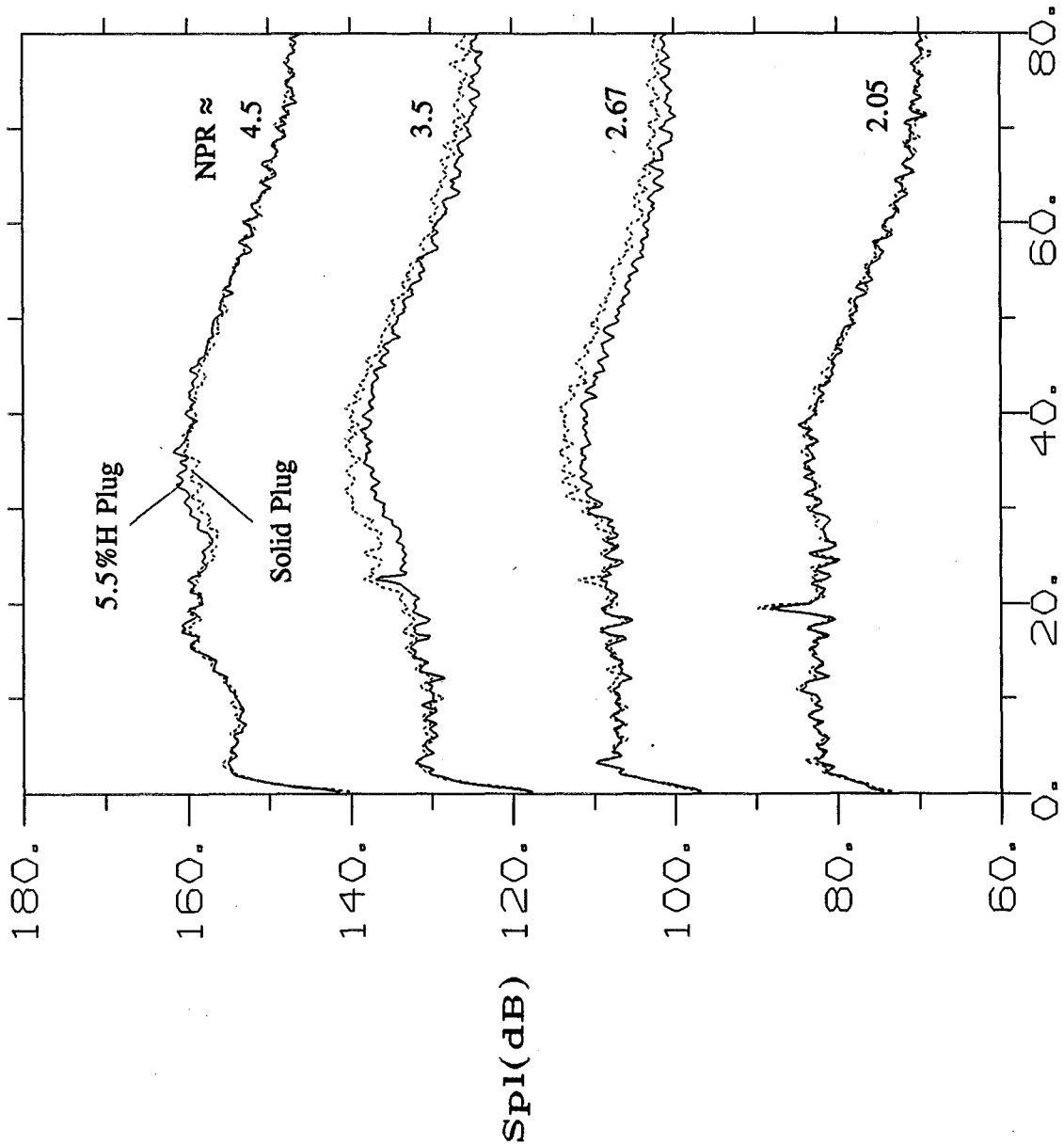
Time 13:23:03

rec	Mj	scr-f	scr-a	oaspl:
330	1.047	19.50	89.8	98.2
328	1.041	22.00	94.5	98.5
329	1.263	40.50	94.2	108.4
325	1.261	10.75	105.2	114.0
315	1.455	32.00	100.6	116.6
306	1.448	22.00	100.9	116.4
302	1.621	37.75	100.6	117.5
290	1.619	7.50	115.1	123.3

plot on 5-OCT-1994

[zaman.ssj] read-spect

FAR FIELD NOISE
 5.5%H PLUG AND SOLID PLUG DATA (WITH 12_4% TAB)
 AT FOUR MACH NUMBERS



Nozzle 8

Date 27-SEP-1994

Time 14:02:39

rec	Mj	scr_f	scr_a	oaspl:
392	1.046	19.50	98.1	98.0
330	1.047	19.50	89.8	98.2
331	1.272	33.25	91.6	106.6
329	1.263	40.50	94.2	108.4
316	1.447	38.25	98.7	114.0
315	1.456	32.00	100.6	116.6
303	1.623	36.00	101.8	118.3
302	1.621	37.75	100.6	117.5

plot on 5-OCT-1994

[zaman.ssj] read_spect

FIG. B16

Nozzle 5

Date 17-NOV-1994

Time 13:47:17

rec	Mj	sr-f	sr-a	oaspl:
334	1.623	18.00	106.6	122.9
343	1.625	34.00	101.6	118.7
334	1.623	18.00	106.6	122.9
344	1.625	7.50	113.7	124.1
334	1.623	18.00	106.6	122.9
335	1.625	12.75	117.1	125.9
333	1.622	16.25	105.2	121.6
336	1.623	12.75	124.1	129.0

plot on 17-NOV-1994

[zaman.ssj] read-spect

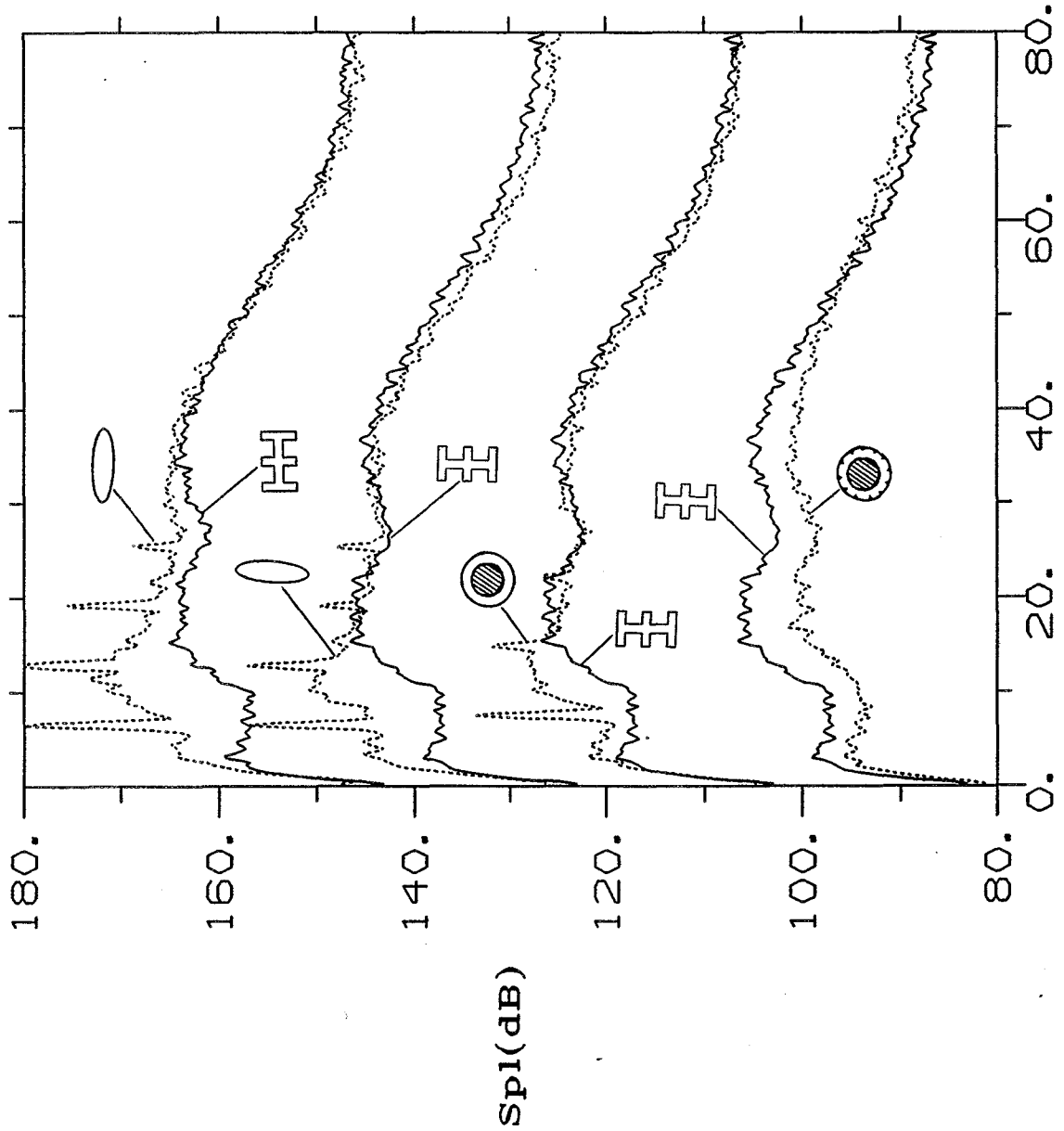


FIG. B17

REPORT DOCUMENTATION PAGE			<i>Form Approved</i> <i>OMB No. 0704-0188</i>	
Public reporting burden for this collection of information is estimated to average 1 hour per response, including the time for reviewing instructions, searching existing data sources, gathering and maintaining the data needed, and completing and reviewing the collection of information. Send comments regarding this burden estimate or any other aspect of this collection of information, including suggestions for reducing this burden, to Washington Headquarters Services, Directorate for Information Operations and Reports, 1215 Jefferson Davis Highway, Suite 1204, Arlington, VA 22202-4302, and to the Office of Management and Budget, Paperwork Reduction Project (0704-0188), Washington, DC 20503.				
1. AGENCY USE ONLY (Leave blank)		2. REPORT DATE March 2001	3. REPORT TYPE AND DATES COVERED Technical Memorandum	
4. TITLE AND SUBTITLE Effect of Delta Tabs on Free Jets from Complex Nozzles			5. FUNDING NUMBERS WU-708-90-43-00	
6. AUTHOR(S) K.B.M.Q. Zaman				
7. PERFORMING ORGANIZATION NAME(S) AND ADDRESS(ES) National Aeronautics and Space Administration John H. Glenn Research Center at Lewis Field Cleveland, Ohio 44135-3191			8. PERFORMING ORGANIZATION REPORT NUMBER E-12601	
9. SPONSORING/MONITORING AGENCY NAME(S) AND ADDRESS(ES) National Aeronautics and Space Administration Washington, DC 20546-0001			10. SPONSORING/MONITORING AGENCY REPORT NUMBER NASA TM-2000-210674	
11. SUPPLEMENTARY NOTES Responsible person, K.B.M.Q. Zaman, organization code 2600, 216-433-5888.				
12a. DISTRIBUTION/AVAILABILITY STATEMENT Unclassified - Unlimited Subject Category: 02 Available electronically at http://gltrs.grc.nasa.gov/GLTRS This publication is available from the NASA Center for AeroSpace Information, 301-621-0390.			12b. DISTRIBUTION CODE	
13. ABSTRACT (Maximum 200 words) Effects of 'delta-tabs' on the mixing and noise characteristics of two model-scale nozzles have been investigated experimentally. The two models are (1) an eight-lobed nozzle simulating the primary flow of a mixer-ejector configuration considered for the HSCT program, (2) an axisymmetric nozzle with a centerbody simulating the 'ACE' configuration also considered for the HSCT program. Details of the flow-field for model (1) are explored, while primarily the noise-field is explored for model (2). Effects of different tab configurations are documented.				
14. SUBJECT TERMS Mixing; Noise; Tabs; Lobed nozzle			15. NUMBER OF PAGES 69	
			16. PRICE CODE A04	
17. SECURITY CLASSIFICATION OF REPORT Unclassified	18. SECURITY CLASSIFICATION OF THIS PAGE Unclassified	19. SECURITY CLASSIFICATION OF ABSTRACT Unclassified	20. LIMITATION OF ABSTRACT	